The first application of a numerically-exact, higher-order sensitivity analysis approach for atmospheric modelling: implementation of the hyperdual-step method in the Community Multiscale Air Quality Model (CMAQ) version 5.3.2

Jiachen Liu[1], Eric Chen[1], Shannon L. Capps[1]

[1]Department of Civil, Architectural & Environmental Engineering, Drexel University, Philadelphia, Pennsylvania, USA

Correspondence to: Shannon L. Capps (shannon.capps@drexel.edu)

Abstract. Sensitivity analysis in chemical transport models quantifies the response of output variables to changes in input parameters. This information is valuable for researchers in data assimilation and model development. Additionally, environmental decision-makers depend upon these expected responses of concentrations to emissions when designing and justifying air pollution control strategies. Existing sensitivity analysis methods include the finite-difference method, the direct decoupled method (DDM), the complex variable method, and the adjoint method. These methods are either prone to significant numerical errors when applied to non-linear models with complex components (e.g., finite difference and complex step methods) or difficult to maintain when the original model is updated (e.g., direct decoupled and adjoint methods). Here, we present the implementation of the hyperdual-step method in the Community Multiscale Air Quality Model (CMAQ) version 5.3.2 as CMAQ-hyd. CMAQ-hyd can be applied to compute numerically exact first- and second-order sensitivities of species concentrations with respect to emissions or concentrations. Compared to CMAQ-DDM and CMAQ-adjoint, CMAQ-hyd is more straightforward to update and maintain while it remains free of ~~numerical~~subtractive cancellation and truncation errors as those augmented models do. To evaluate the accuracy of the implementation, the sensitivities computed by CMAQ-hyd are compared with those calculated with other traditional methods or a hybrid of the traditional and advanced methods. We demonstrate the capability of CMAQ-hyd with the newly implemented gas-phase chemistry and biogenic aerosol formation mechanism in CMAQ. We also explored the cross-sensitivity of monoterpene nitrate aerosol formation to its anthropogenic and biogenic precursors to show the additional sensitivity information computed by CMAQ-hyd. Compared with the traditional finite difference method, CMAQ-hyd consumes fewer computational resources when the same sensitivity coefficients are calculated. This novel method implemented in CMAQ is also computationally competitive with other existing methods and could be further optimised to reduce memory and computational time overheads.

1 Introduction

Ambient air pollution, including particulate matter (PM), poses significant threats to human health. According to the Global Burden of Disease study, ambient PM pollution accounted for 4.7 % of the Disability-Adjusted Life Years among all risk factors (Murray et al., 2020) and over 4.1 million deaths (Fuller et al., 2022) in 2019. Therefore, understanding the complex physicochemical and atmospheric transport processes that lead to PM formation is essential to reducing PM and other harmful secondary atmospheric pollutants. Amongst atmospheric scientists, chemical transport models (CTMs) have become essential tools for interpreting observations of and examining inferences about formation processes of atmospheric pollutants. By solving the mass conservation equation for different species based on atmospheric dispersion and transport, photochemical processes, atmospheric chemistry, and aerosol processes, CTMs can provide estimates of primary and secondary air pollutants (Seinfeld and Pandis, 2016). Environmental decision-makers and researchers rely on CTMs to determine appropriate policies to control air pollution and predict atmospheric pollutant concentrations. Experimental studies (e.g., Ng et al., 2008) and measurement campaigns (e.g., Sareen et al., 2016) provide researchers with more insights about the anthropogenic and biogenic aerosol formation processes. These studies ultimately lead to developments and updates to the gas-phase chemistry and aerosol formation mechanisms in CTMs. For these newly added species and mechanisms in CTMs, understanding the sensitivity of aerosol species concentration with respect to their precursor emissions is crucial for determining the priority of primary pollutant emission reductions to achieve atmospheric pollutant reduction objectives.

Sensitivity analysis methods have become invaluable for evaluating uncertainties, understanding concentration-emission relationships in CTMs, and assimilating observations of atmospheric pollutants to improve model parameters. Specifically, the kind of sensitivities here described are the partial derivative of one or more model outputs with respect to one or more model inputs. For instance, if the model has input variables as $\boldsymbol{X}$ and output variables as $\boldsymbol{Y}$, the n^{th}-order sensitivity coefficient of one output variable Y_i to one input variable X_i can be represented as the n^{th}-order partial derivative of Y_i to X_i, $\frac{\partial^n Y_i}{\partial X_i^n}$ (Cohan and Napelenok, 2011). Most sensitivity analysis techniques are formulations of the tangent linear model which provides source-oriented sensitivities or, mathematically, one column of the Jacobian or Hessian at the model state. In contrast, the model adjoint provides receptor-oriented sensitivities or, mathematically, one row of the Jacobian at the model state. Two distinct approaches to developing these models are the continuous approach, in which the derivative of the underlying equation is formulated and then implemented numerically, and the discrete approach, in which the derivative of the numerical solution of the model is formulated (Sandu et al., 2005). Since the model adjoint provides source-oriented sensitivities and is not directly comparable with other methods, including the hyperdual-step method, which is the focus of this work, it will not be further discussed in the following sections. Other augmented model methods including the Integrated Source Apportionment Method (Kwok et al., 2013; Kwok et al., 2015) is based on a different approach thus also not discussed further in the following paragraphs.

The first-order sensitivity coefficient is usually the most useful for CTM applications because it describes the linear relationship between X_i and Y_i. Higher-order sensitivities can be helpful when assessing the nonlinear relationships or dynamics

among multiple input variables. Previous studies found that highly nonlinear concentration-emission responses commonly exist in CTMs, particularly for the formation process of PM (Hakami, 2004; Xu et al., 2018; Tian et al., 2010). Therefore, accurately determining the first-order and second-order relationships are useful for understanding concentration-emission responses in CTMs. Practically, the characteristics of an ideal sensitivity analysis method are numerical accuracy, computational efficiency, and minimal development (Lantoine et al., 2012).

Because analytical sensitivities are impractical for these models, researchers have employed a few numerical methods to calculate the first- and higher-order sensitivities in CTMs. One such method is the finite difference method (FDM), which is often designated the brute-force method. The FDM is based on the first- or higher-order approximation of the Taylor series expansion from a small perturbation (Boole, 1960). The sensitivities are calculated by running the model multiple times with incrementally different values for the input variables of interest and taking the difference of the resulting concentration fields. While this method is simple to understand and implement, truncation and subtractive cancellation errors can substantially reduce the accuracy of the calculated sensitivity coefficients, particularly for nonlinear input-output relationships (Fornberg, 1981). Truncation errors originate from neglected higher-order terms in the Taylor series expansion. For instance, suppose a policymaker is interested in calculating the effects of reducing SO_2 emission on the total $PM_{2.5}$ concentration. The sensitivity analysis indicates that the first-order partial derivative is positive, and the second-order partial derivative is negative. In that case, only considering the first-order FDM approximation will overestimate the effect of reducing SO_2 emission on the total $PM_{2.5}$ concentration. The truncation error can be minimised by taking a small perturbation step, thus eliminating the impact of higher-order sensitivity terms on the first-order result. However, smaller perturbation steps might lead to subtractive cancellation errors, which stem from the fact that computers cannot distinguish two numbers close to each other. If the perturbation size is within the numerical noise of the model, the numerator difference sometimes approaches zero or the sensitivity information might be meaningless, which causes an inherent tension between reducing the truncation error and subtractive cancellation error for the FDM. Determining ideal perturbation sizes for different variables is challenging because the ideal perturbation size depends on the input species of interest and other parameters in the model. The necessity of selecting the proper perturbation size for each input variable of interest and running the model multiple times makes the FDM a computationally expensive method to obtain sufficiently accurate sensitivities from CTMs.

As a continuous, source-oriented approach, the decoupled direct method (DDM) eliminates the numerical accuracy issues of the FDM and improves the computational efficiency of calculating source-oriented sensitivities but only with a hefty development cost. ~~Dunker (1981)~~Dunker (1981) introduced to atmospheric modelling the direct method, which involves formulating new sensitivity equations from the original model and solving both sets simultaneously. The direct method has been proven numerically unstable for solving stiff equations, which exist in many chemical transport models~~ (Yang et al., 1997).~~. On the other hand, DDM formulates sensitivity equations like the direct method but separately solves the original and sensitivity equations~~, which improves the computational efficiency and stability over the direct method. Dunker et al. (2002) developed DDM-3D and applied it to a three-dimensional air quality~~. This approach improves the computational efficiency and stability compared to the direct method. Yang et al. (1997) was the first to apply the DDM-3D method in a three-

dimensional chemical transport model. Hakami et al. (2003) ~~applied~~ extended the method to a higher-order DDM (HDDM) in the gas phase of the Community Multiscale Air Quality Model (CMAQ), while Zhang et al. (2012) augmented CMAQ-HDDM to include the second-order sensitivities of $PM_{2.5}$ concentration to NO_x and SO_2 emissions. Unlike the FDM, the DDM does not incur truncation or subtractive cancellation errors since separate equations are solved for the sensitivities. The DDM also allows the computation of sensitivities of many outputs to more than one input simultaneously, saving significant computation resources. The major disadvantage of DDM for CMAQ and other CTMs is the difficulty of co-development alongside ongoing scientific model development, which is one purpose of CTMs. The implementation of DDM requires writing sensitivity equations for nonlinear steps, which commonly exist in the chemistry and advection parts of CTMs (Fike and Alonso, 2011). New sensitivity equations must be written when CTMs are updated, reducing the ease of maintenance of DDM in complex CTMs and eliminating the opportunity for sensitivities to be used for evaluation in the process of developing new scientific modules within the CTMs.

The complex variable method (CVM) and the multicomplex step approach (MCX) are the methods most comparable to the hyperdual step method. Lyness and Moler (1967) introduced the concept of using imaginary space to propagate derivatives for functions in real space based on Cauchy integrals. ~~Squire and Trapp (1998)~~Squire and Trapp (1998) made the idea practical through an elegant truncation of the Taylor series expansion of complex numbers, which allows nearly exact first-order sensitivities if the imaginary perturbation is small enough. ~~Constantin and Barrett (2014)~~Constantin and Barrett (2014) applied CVM on the adjoint method of the global CTM GEOS-Chem to compute near-exact sensitivities with receptor-orientation in one order and source-orientation in the other. Lantoine et al. (2012) developed a multicomplex number system to allow higher-order sensitivities to be calculated to machine precision for functions in real space. Berman et al. (2023) implemented MCX in the inorganic aerosol thermodynamic model, ISORROPIA, which is used in CMAQ and other air quality models. These methods require inclusion of a library of overloaded operators to treat the types of numbers required and conversion of the model from real to complex space. The accuracy of these approaches is only limited by ensuring that the imaginary perturbation is small enough, which may require tuning depending on the complexity of the model. CVM does not require as much more memory and computational time as MCX, but both contribute overhead. Both are very easily updated with new scientific modules. The main limitation of CVM and MCX is that sensitivities cannot be propagated through models, like CMAQ, that originally include calculations in imaginary space.

Finally, the method of interest in this work is the hyperdual-step method (HYD), which computes source-oriented first- and second-order sensitivities to machine precision. HYD relies on hyperdual numbers, which are a specific type of generalised complex number developed particularly for first- and second-order derivative calculations (Fike and Alonso, 2011). The HYD, like the CVM or MCX, is an approach based on a Taylor series expansion in a non-real number space. The unique mathematical properties of hyperdual numbers lead to an elegant calculation of first-, second-, and potentially higher-order sensitivities to machine precision without truncation or cancellation errors. Hyperdual numbers have been applied in numerical models in different fields of study to calculate exact first- and second-order derivatives. Cohen and Shoham (2015) applied hyperdual numbers to compute second-order derivatives in multibody kinetics problems. Tanaka et al. (2015) utilized

hyperdual numbers to automatically differentiate hyperelastic material models. Rehner and Bauer (2021) applied hyperdual numbers to equation of state ~~modeling~~modelling and the calculation of critical points. This method, which is applicable to models with calculations in imaginary space, is accurate to machine precision, reasonably computationally expensive, and quite straightforward to update.

Here, we implement the HYD in CMAQ version 5.3.2 to develop the novel augmented model, CMAQ-hyd, and apply it to calculate the sensitivities both inorganic and organic aerosol concentration with respect to their precursor emissions. To our best knowledge, this work represents the first implementation of hyperdual numbers to calculate first- and second-order sensitivities in a CTM. In Section 2, hyperdual numbers and the hyperdual-step method are introduced as well as the process of implementing and evaluating HYD in CMAQ. In Section 3, the evaluation of first- and second-order sensitivities from CMAQ-hyd is conducted, including the computational costs. In Section 4, CMAQ-hyd is applied to understand the influences of anthropogenic and biogenic emissions on select secondary organic aerosol (SOA) concentrations. This work provides an accurate and easily manageable method to compute first- and second-order sensitivities implemented in CMAQ version 5.3.2 and an example of potential application in other complex models where the sensitivities are of interest.

2 Methods

2.1 Hyperdual numbers and the hyperdual-step method

A hyperdual number (Fike and Alonso, 2011) has four components and is characterised by

$$H = a_0 + a_1\epsilon_1 + a_2\epsilon_2 + a_{12}\epsilon_{12} \quad (1)$$

where a_0, a_1, a_2, and a_{12} are real numbers, and ϵ_1, ϵ_2, and ϵ_{12} are non-real parts. The three crucial properties which enable numerically exact first- and second-order sensitivity calculations are:

$$\epsilon_1^2 = \epsilon_2^2 = \epsilon_{12}^2 = 0 \quad (2)$$

$$\epsilon_1 \neq \epsilon_2 \neq \epsilon_{12} \neq 0 \quad ~~(2)~~(3)$$

$$\epsilon_1\epsilon_2 = \epsilon_{12} \quad ~~(3)~~(4)$$

The squares of the non-real individual parts equal zero (Eq. 2). The non-real parts themselves do not equal anything in real space (Eq. 3). The multiplication of ϵ_1 and ϵ_2 is equal to the third non-real component ϵ_{12} (Eq. 4). The addition and multiplication of hyperdual numbers are commutative, and the definitions help eliminate the higher-order terms in a Taylor series expansion. A demonstration of several basic operations is provided in the SI while a more detailed discussion of the mathematical properties of hyperdual numbers is given by Fike and Alonso (2011).

~~The~~Akin to the Taylor series expansion about the real value of x in the finite difference method, the method of ascertaining sensitivities through a perturbation in ~~non real~~hyperdual space is based on ~~multiplying~~a Taylor series expansion in an orthogonal dimension of the number. Specifically, a hyperdual number with unity in a_0 and unity in one of a_1~~,~~ or a_2~~,~~ ~~and a_{12}~~ is multiplied with the independent variable of interest. After model execution, a Taylor series expansion is applied to

extract sensitivities. ~~The~~For instance, the hyperdual-step method is applied to a scalar function $f(x)$ by multiplying x by the hyperdual number $H_h = 1.0 + h_1\epsilon_1 + h_2\epsilon_2$ ~~and~~, which results in

$$f(xH_h) = f(x) + (xh_1\epsilon_1 + xh_2\epsilon_2)f'(x) + \frac{1}{2!}(xh_1\epsilon_1 + xh_2\epsilon_2)^2 f''(x) + \frac{1}{3!}(xh_1\epsilon_1 + xh_2\epsilon_2)^3 f'''(x) + \cdots \quad (5)$$

where "…" represents higher order terms in the series. Eliminating all terms that are zero due to the definition of hyperdual numbers (Eq. 2~~),~~) leads to

$$f(xH_h) = f(x) + (xh_1\epsilon_1 + xh_2\epsilon_2)f'(x) + x^2 h_1 h_2 \epsilon_{12} f''(x) \quad (6)$$

where $f(xH_h)$ is a hyperdual number.

The properties of hyperdual numbers (Eqs. 2–4) lead to two significant results. First, all terms in the Taylor series expansion with derivatives higher than second-order become zero because all values include ~~either ϵ_1^2, ϵ_2^2, or ϵ_{12}^2. Second, the real component is unchanged.~~ ϵ_1^2, ϵ_2^2, or ϵ_{12}^2. Second, the real component is unchanged. A more detailed expansion of terms can be found in Eq. S7 in the SI or the original development of hyperdual numbers, following the multiplication rule between a hyperdual and a real number (Fike and Alonso, 2011). Finally, the first- and second-order derivatives are separated into different parts of the hyperdual number. The first-order derivative exists in either the ϵ_1 or the ϵ_2 term, while the second-order derivatives only exist in the ϵ_{12} term. The first and second-order derivatives are,

$$f'(x) = \frac{\epsilon_1 part[f(xH_h)]}{xh_1} = \frac{\epsilon_2 part[f(xH_h)]}{xh_2} \quad (7)$$

$$f''(x) = \frac{\epsilon_{12} part[f(xH_h)]}{x^2 h_1 h_2} \quad (8)$$

where $\epsilon_1 part[]$, $\epsilon_2 part[]$, and $\epsilon_{12} part[]$ represent functions that extract the a_1, a_2, or a_{12}, respectively. Since the derivative computation process (Eqs. 6–9) does not involve subtractions or higher-order sensitivities, the first- and second-order sensitivities calculated by the hyperdual-step method are free from subtractive cancellation and truncation errors. This method (Eqs. 8–9) extends to vector operations to compute arrays of numerically exact derivatives. For instance, the partial first- and second-order derivatives for $f(\boldsymbol{x})$, where $\boldsymbol{x} = [x_1, x_2, \ldots, x_n]$, with respect to x_1 through a hyperdual-step perturbation to x_1 is:

$$\frac{\partial f(\boldsymbol{x})}{\partial x_1} = \frac{\epsilon_1 part[f(\boldsymbol{x}H_{h,x_1})]}{x_1 h_1} = \frac{\epsilon_2 part[f(\boldsymbol{x}H_{h,x_1})]}{x_1 h_2} \quad (9)$$

$$\frac{\partial^2 f(\boldsymbol{x})}{\partial x_1^2} = \frac{\epsilon_{12} part[f(\boldsymbol{x}H_{h,x_1})]}{x_1^2 h_1 h_2} \quad (10)$$

Similarly, two different independent variables x_1 and x_2 may be perturbed simultaneously. In this case, two arrays of first-order sensitivity and one array of cross-sensitivity result as:

$$\frac{\partial f(\boldsymbol{x})}{\partial x_1} = \frac{\epsilon_1 part[f(\boldsymbol{x}) * H_h]}{x_1 h_1} \tag{11}$$

$$\frac{\partial f(\boldsymbol{x})}{\partial x_2} = \frac{\epsilon_2 part[f(\boldsymbol{x}) * H_h]}{x_2 h_2} \tag{12}$$

$$\frac{\partial^2 f(\boldsymbol{x})}{\partial x_1 \partial x_2} = \frac{\epsilon_{12} part[f(\boldsymbol{x}) * H_h]}{x_1 x_2 h_1 h_2} \tag{13}$$

Therefore, the two variations of the hyperdual-step method will generate either one or two arrays of first-order sensitivities and one array of second-order or cross sensitivities with a single run of the model.

2.2 Community Multiscale Air Quality Model and the implementation of the hyperdual-step method

The Community Multiscale Air Quality model (CMAQ) developed by the US EPA is an Eulerian CTMs which can predict air pollutant concentrations on regional and hemispheric scales (Byun and Schere, 2006). CMAQ represents advection, diffusion, gas-phase chemistry, aerosol processes, cloud processes, and photolysis. CMAQ has been applied to predict pollutant concentrations in the atmosphere (Liu et al., 2010; ~~Sayeed et al., 2021~~Sayeed et al., 2021), understand fundamental atmospheric chemistry and aerosol formation mechanisms (Zhu et al., 2018; Li et al., 2019), and guide policy-making processes ~~(Chemel et al., 2014; Che et al., 2011; ~~(Chemel et al., 2014; Che et al., 2011; Li et al., 2019~~; Ring et al., 2018); Ring et al., 2018)~~. CMAQ is used in the regulatory process of the US EPA when states, tribes, or local jurisdictions demonstrate how they will attain the National Ambient Air Quality Standard (NAAQS) and or comply with the Regional Haze Rule (Mebust et al., 2003). CMAQ solves the atmospheric diffusion equation shown in Eq. (14) to calculate the concentrations of gaseous and aerosol species in the atmosphere.

$$\frac{\partial c_i}{\partial t} = -\nabla(\boldsymbol{u} c_i) + \nabla(\boldsymbol{K} \nabla c_i) + R_i + E_i \tag{14}$$

where c_i, $\boldsymbol{u}$, $\mathbf{K}$, R_i and E_i are the concentration of species i, the wind velocity vector, the diffusivity tensor, the change in concentration due to chemical reaction of species i, and the emissions rate of species i, respectively. Species concentrations are stored in a multidimensional array and propagated through different scientific modules within the model. For this work, CMAQ was run with 12 km by 12 km horizontal resolution with 35 vertical layers, 100 columns, and 80 rows over the Southeast US on July 1st, 2016, GMT ~~(U.S. Environmental Protection Agency, 2019)~~(U.S. Environmental Protection Agency, 2019) . The gas-phase chemistry mechanism used is Carbon Bond 6 (Luecken et al., 2019).

In CMAQ, the hyperdual-step method was implemented by strategically converting the model to use hyperdual numbers (Figure 1). First, the operators were overloaded by translating a C-based library from Fike and Alonso (2011) to Fortran ("HDMod") and augmenting it to treat multidimensional data as required by CMAQ. HDMod, which defines a hyperdual version of all possible calculations related to the chemical concentration array, was developed. The library includes basic arithmetic operations, such as addition and subtraction, as well as more advanced functions like trigonometric functions.

Before being applied to CMAQ, the operator overloading library was separately ~~tested~~validated by comparing against analytical derivatives using a testing framework developed by Pellegrini and Russell (2016). Secondly, the CMAQ variable containing species concentration information and all other variables that depend on it were converted from real numbers to the newly defined hyperdual number type. The source code was carefully analysed to select only the necessary variables for conversion. Many variables in CMAQ do not need to be altered because they do not influence the main concentration array. This highly detailed process helped minimise the additional computational burden of the model since calculations with hyperdual numbers are more computationally intensive than those with real numbers. For instance, one hyperdual multiplication operation shown in Eq. (5) results in five more additions and nine more multiplications than an operation with real numbers. According to Fike and Alonso (2011), the computational cost of a hyperdual calculation ranges from 4 to 14 times higher than the original operation. Applying hyperdual numbers to all the variables in a CFD model results in approximately 10 times higher computational cost (Fike and Alonso, 2011). Thirdly, the first- and second-order sensitivities of the species concentrations to perturbed emissions are included in the new hyperdual array, which is then saved to additional output files using the same structure as the output of the original concentration array. As a result, first- and second-order sensitivities can be propagated through the model without significantly modifying the source code. The modification efforts mainly focused on determining the variables that must be converted to the hyperdual type. Consequently, updating CMAQ-hyd when there are changes to the original model is a simple process that involves converting only the newly added variables to the hyperdual type. This simplicity is an advantage over other computational techniques, such as the DDM and adjoint

method, which compute numerically exact sensitivities but require more complex and time-consuming update procedures, including writing new equations.

~~Some~~Several source code ~~alternations~~alterations were made to reduce the complexity of development and overcome the numerical instabilities related to hyperdual calculations in CMAQ's aerosol module~~. CMAQ uses~~, specifically within the inorganic thermodynamic module ISORROPIA~~ to compute the partitioning of inorganic aerosol and gas-phase species~~ (Fountoukis and Nenes, 2007; Nenes et al., 1998). For the simplicity of development, we applied a Fortran 90-compilant version of ISORROPIA ~~can run~~to replace the original Fortran 77 version of ISORROPIA in CMAQ.

ISORROPIA, as a key component of the aerosol module in CMAQ, is called either in the forward or the reverse

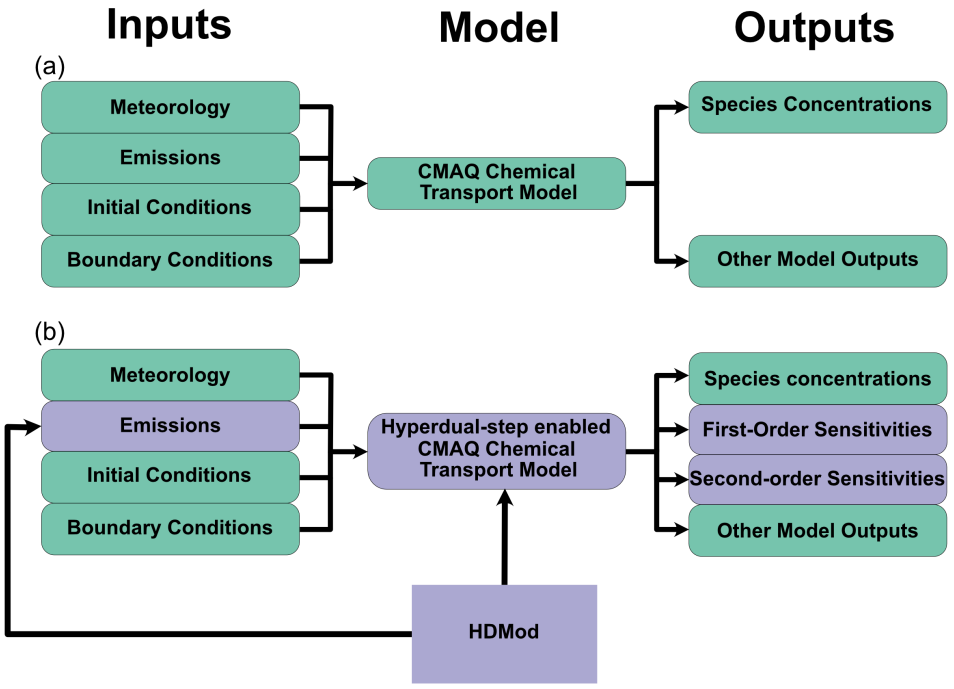

~~**Fig 1.** A schematic showing the original CMAQ model compared with the CMAQ-hyd. **(a)** The original CMAQ model (green). **(b)** The CMAQ-hyd model. The CMAQ-hyd incorporates a hyperdual number overloading modules. The purple components in (b) represent changes made to the original CMAQ model. Changes were made to the modules and emission processing parts of CMAQ. The first- and second-order sensitivities of species concentrations with respect to selected precursor concentrations or emissions are new outputs of the model.~~

mode. The forward mode of ISORROPIA takes the sum of gas and aerosol species concentrations, along with the relative humidity and temperature, to determine the partitioning of ~~species in either the gas or aerosol phase. The reverse mode of ISORROPIA starts with known concentrations of aerosol species and can output the species concentration in the solid, liquid, and gas phases. CMAQ uses the reverse mode to compute the thermodynamics of coarse-mode inorganic aerosols.~~ Aitken- and accumulation-mode species across the gas and aerosol phases in CMAQ.~~The reverse mode solution leads to unrealistic sensitivities calculated by the HYD when the aerosol pH is close to neutral. One previous study found that the reverse~~

~~ISORROPIA fails to capture the actual behaviour of inorganic aerosol when the pH is close to 7 (Hennigan et al., 2015), and the necessary change was to ignore the sensitivity calculations in CMAQ when the pH of coarse mode aerosol is close to neutral. The original implementation was numerically unstable during iterations for upper-layer cells with low temperature and pressure in the forward-mode inorganic aerosol computation for Aitken-mode and fine-mode aerosols.~~ In the original CMAQ model, ISORROPIA is run in the forward mode without limiting the temperature and pressure of the simulation. The determination process of species concentrations involves an iterative method which sometimes is numerically unstable during iterations for upper layer cells with low temperature and pressure~~. The~~ for sensitivity computations with the HYD. To increase the numerical stability of CMAQ-hyd, we implemented temperature and pressure constraints so that the forward-mode ISORROPIA is only called when the cell temperature exceeds 260 K, and cell pressure exceeds 20,000 Pa ~~to increase the numerical stability of the model.~~ A similar set of temperature and pressure limits was applied to the call of ISORROPIA in the adjoint of CMAQ (Zhao et al., 2020). These changes do not affect the species concentrations computed by CMAQ ~~and ensure~~while ensuring that the sensitivity computation process is stable. ~~For the simplicity of development, we applied a Fortran 90-compliant version of ISORROPIA to CMAQ-hyd.~~

To calculate the dynamic equilibrium of coarse mode aerosol species with the gas phase (Pilinis et al., 2000; Capaldo et al., 2000), CMAQ employs the reverse mode of ISORROPIA. The input to reverse mode ISORROPIA includes concentrations of aerosol species, relative humidity, and temperature, and it results in partitioned concentrations in the solid, liquid, and gas phasesfor coarse-mode inorganic aerosols. The reverse-mode solution leads to unrealistic sensitivities calculated by the HYD when the aerosol pH is close to neutral. One previous study found that the reverse ISORROPIA fails to capture the actual behaviour of inorganic aerosol when the pH is close to 7 (Hennigan et al., 2015). To ensure the stability of the sensitivity calculations, the changes to the hyperdual components in the coarse mode dynamic equilibrium are ignored when the pH of coarse mode aerosol is close to neutral, which ensures that the real components are identical to the original model.

2.3 Evaluating sensitivities from CMAQ-hyd

CMAQ-hyd produces sensitivities that can be semi- or fully-normalized for concentrations from any range of grid cells and times with respect to emissions or concentrations from any range of grid cells and times. Here, for the sake of illustration, we consider the semi-normalised sensitivities of time-averaged output concentrations ~~on the~~of ground ~~layer~~-level $PM_{2.5}$ concentrations, $C_{PM_{2.5},c,r,l=0,t}$, to input NO_x ($NO+NO_2$) emissions, $E_{NO_x,c,r,l,t}$, averaged over time, ~~which would be a typical application for an environmental decision maker~~*t*, for any given cell as indicated by the column, *c*, and row, *r*. First-order semi-normalized sensitivities, $s_{NO_x}^{PM_{2.5}}$, and second-order semi-normalised sensitivities, $s_{NO_x}^{(2)PM_{2.5}}$~~, of $PM_{2.5}$ concentrations, $C_{PM_{2.5}}$, to NO_x ($NO+NO_2$) emissions, E_{NO_x},~~ exemplify sensitivities relevant to environmental decision makers (Eqs. 15–16~~–17~~).

$$s_{NO_x}^{PM_{2.5}} = \frac{\partial C_{PM_{2.5}}}{\partial E_{NO_x}} E_{NO_x} s_{NO_x}^{PM_{2.5}} = \frac{\partial \overline{C_{PM_{2.5},c,r,l=0,t}}|_t}{\partial \overline{E_{NO_x,c,r,l,t}}|_t} \overline{E_{NO_x,c,r,l,t}}|_t \quad (1615)$$

$$s_{NO_x}^{(2)PM_{2.5}} = \frac{\partial^2 C_{PM_{2.5}}}{\partial E_{NO_x}^2} E_{NO_x}^2 s_{NO_x}^{(2)PM_{2.5}} = \frac{\partial^2 \overline{C_{PM_{2.5},c,r,l=0,t}}|_t}{\partial \overline{E_{NO_x,c,r,l,t}^2}|_t} \overline{E_{NO_x,c,r,l,t}^2}|_t \quad (1716)$$

Semi-normalised sensitivities reduce the complexity of interpretation by providing sensitivities in the units of the concentration per percent change of emissions. Here, $C_{PM_{2.5}}$ and E_{NO_x} are the concentration of $PM_{2.5}$ and emission of NO_x at a given cell in the modelling domain each averaged in time, respectively. The semi-normalised sensitivities also scale down the impact from cells with low emission rates, which is consistent with the concentration reduction that is realistic to expect. Similarly, the time-averaged, semi-normalised cross-sensitivity of $PM_{2.5}$ to both NO_x and monoterpene is denoted as $s_{NO_x,TERP}^{(2)PM_{2.5}}$, with E_{TERP} representing the emission of monoterpenes (Eq. 1817).

$$s_{NO_x,TERP}^{(2)PM_{2.5}} = \frac{\partial^2 C_{PM_{2.5}}}{\partial E_{NO_x} \partial E_{TERP}} (E_{NO_x} E_{TERP}) s_{NO_x,TERP}^{(2)PM_{2.5}} = \frac{\partial^2 \overline{C_{PM_{2.5},c,r,l=0,t}}|_t}{\partial \overline{E_{NO_x,c,r,l,t}}|_t \overline{E_{TERP,c,r,l,t}}|_t} \overline{E_{NO_x,c,r,l,t}}|_t \overline{E_{TERP,c,r,l,t}}|_t \quad (1817)$$

The evaluation of CMAQ-hyd in first order is done by performing a comparison of the sensitivities calculated by the hyperdual-step method against those from the FDM (Eq. 1918). The comparison is illustrated with an example of calculating cell-specific sensitivities of $PM_{2.5}$ concentration to NO_x emissions. The first-order sensitivity of $PM_{2.5}$ concentration at the end of a 24-hour simulation to cumulative NO_x emission perturbation is given by

$$s_{NO_x}^{PM_{2.5},t=24} \approx \frac{C_{PM_{2.5},c,r,l,t=24}^{inc} - C_{PM_{2.5},c,r,l,t=24}^{dec}}{\sum_{t=0}^{t=24} E_{NO_x,c,r,l=0,t}^{inc} - \sum_{t=0}^{t=24} E_{NO_x,c,r,l=0,t}^{dec}} \Sigma_{t=0}^{t=24} E_{NO_x,c,r,l=0,t}^{orig} \quad (1918)$$

where the subscripts *c*, *r*, and *l* represent the column, row, and layer; the subscript *t* represents the time from the start of the model run; and the superscripts *inc*, *dec*, and *orig* represent the initial perturbation direction (i.e., increased, decreased, and original emissions, respectively). For instance, $C_{PM_{2.5},c,r,l,t=24}^{inc}$ is the concentration of $PM_{2.5}$ for each column, row, and layer at 24 hours into the run, with an increase in NO_x emissions throughout the model run. Unless otherwise noted, the relative perturbation size for first-order FDM calculations is 125 % and 75 % for domain-wide emissions. The average ground-layer sensitivities for the 24-hr simulation time are computed. Previous studies have found smaller perturbation sizes for inorganic aerosol sensitivity calculations in CMAQ using FDM are more prone to numerical noise (Zhang et al., 2012). The semi-normalised sensitivity of each cell is computed with the central difference method and is only an approximation of the actual sensitivities due to subtractive cancellation and truncation errors. The numerator is the difference between $PM_{2.5}$ concentrations with persistent increases or decreases in NO_x emissions. The denominator is the total emission perturbation of NO_x emission. The sensitivities are semi-normalised by the sum of NO_x emissions in the base model run. The calculated first-order semi-normalised sensitivities will have units of μg m^{-3}. Sensitivities calculated with this method (Eq. 19) can only be an approximation due to numerical errors mentioned in Section 2.1.

The semi-normalised sensitivity of $PM_{2.5}$ concentrations with respect to NO_x emissions using a hyperdual perturbation of $H_a = 1 + a_1\epsilon_1 + a_2\epsilon_2$ is computed by the hyperdual-step method as

$$s_{NO_x}^{PM_{2.5},t=24} = \frac{\epsilon_1 part\left[C_{PM_{2.5},c,r,l,t=24}^{orig}\right]}{a_1} = \frac{\epsilon_2 part\left[C_{PM_{2.5},c,r,l,t=24}^{orig}\right]}{a_2} \quad (19)$$

The first-order semi-normalised sensitivity can be computed with either the ϵ_1 or the ϵ_2 part. The ϵ_1 or the ϵ_2 part of the $PM_{2.5}$ concentration divided by the initial perturbation in the ϵ_1 or ϵ_2 space, respectively. The emissions in the denominator will cancel out with the semi-normalised emissions.

Although the FDM can be applied to compute second-order sensitivities in CMAQ, previous studies have shown that the results are noisy and highly dependent on the perturbation sizes (Zhao et al., 2020; Zhang et al., 2012). ~~The~~ In order to evaluate the second-order ~~sensitivity evaluation is between~~sensitivities computed by the HYD method, we adopted a hybrid hyperdual-finite-difference method (HYD-FDM~~) and the hyperdual-step method. The hybrid~~). The HYD-FDM sensitivity calculation is given by:

$$s_{NO_x}^{(2)PM_{2.5}} \approx \frac{\frac{\epsilon_1 part[C_{PM_{2.5},c,r,l,t=24}^{inc}]}{a_1 \sum_{t=0}^{t=24} E_{NO_x,c,r,l=0,t}^{inc}} - \frac{\epsilon_1 part[C_{PM_{2.5},c,r,l,t=24}^{dec}]}{b_1 \sum_{t=0}^{t=24} E_{NO_x,c,r,l=0,t}^{dec}}}{\sum_{t=0}^{t=24} E_{NO_x,c,r,l=0,t}^{inc} - \sum_{t=0}^{t=24} E_{NO_x,c,r,l=0,t}^{dec}} \left(\Sigma_{t=0}^{t=24} E_{NO_x,c,r,l=0,t}^{orig}\right)^2 \quad (20)$$

where two separate simulations were run: one with increased and another with decreased initial NO_x emissions. The perturbation on emissions for two runs is $H_a = 1 + a_1\epsilon_1 + a_2\epsilon_2$ for the run with increased initial NO_x emission, and $H_b = 1 + b_1\epsilon_1 + b_2\epsilon_2$ for the run with decreased initial emission of NO_x. The HYD-FDM uses the regular finite difference on the difference between first-order sensitivities calculated by using the ϵ_1 part of the hyperdual-step results. The sensitivity in this equation is an estimate and subject to numerical errors because it includes the usage of FDM.

The second-order sensitivity calculated by the hyperdual-step method is shown in Eq. (21) below.

$$s_{NO_x}^{(2)PM_{2.5}} = \frac{\epsilon_{12} part\left[C_{PM_{2.5},c,r,l,t=24}^{orig}\right]}{a_1 a_2} \quad (21)$$

The hyperdual-step method uses the ϵ_{12} part of the output variable and divide it by the multiplication of a_1 and a_2. The second-order sensitivities calculated only by the HYD method are numerically exact. All the sensitivities are computed for each cell, and comparisons between the finite difference and the hyperdual-step method are performed on a cell-to-cell basis.

3 Results and Discussion

3.1 Evaluation of the first- and second-order sensitivities

We evaluated the implementation of CMAQ-hyd by comparing the first-order sensitivities of various species in CMAQ calculated by HYD with a hyperdual-step perturbation described in Section 2.3 (HYD sensitivities) and FDM with a ~~50%~~ domain-wide emission perturbation (FD sensitivities). The FD sensitivities were computed with the difference between a 25% increase and a 25% decrease in domain-wide emissions using the central finite difference method. Overall, different HYD and FD sensitivities agree well, as evidenced by the close alignment of the points on the blue identity line, which represents perfect agreement, in most panels of Figure 2. The slope and R^2 values for all comparisons are provided in Table 1, and additional slope and R^2 values are provided in Table S1 and Table S2. Specifically, the slopes and R^2 of gas-phase

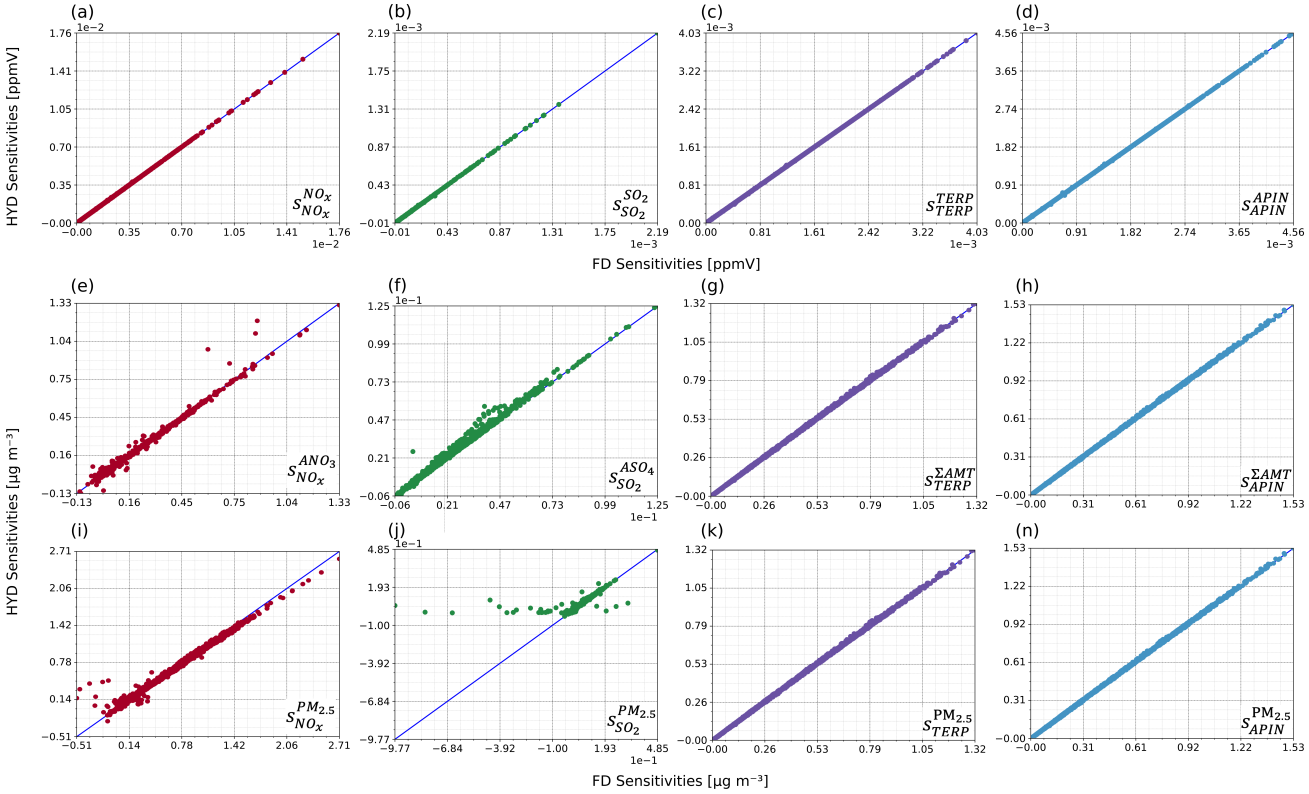

~~**Figure 2.** The comparisons of first-order sensitivities on the ground layer calculated by the hyperdual-step method (HYD sensitivities) and FDM (FD sensitivities). The sensitivities are color-coded by the perturbed emissions (i.e., NO_x, SO_2, TERP, and APIN). (a)–(d) are the gas-phase species sensitivities with respect to their emissions. APIN denotes α-pinene and TERP denotes all other monoterpene species. (e)–(h) are examples of aerosol phase products with respect to their precursors. ANO_3 denotes the total aerosol phase nitrate products. ASO_4 denotes the total aerosol sulphate products. ΣAMT denotes the total aerosol photooxidation products from monoterpene. (i)–(n) are the total $PM_{2.5}$ concentration with respect to gas phase precursors. The sensitivities calculated are noted at the bottom right corner of each panel with the notation pattern mentioned in Section 2.3.~~

species concentration on the ground layer with respect to their emissions on the ground layer (Figs. 2a–2d) are all 1.00 (Table 1), indicating minimal nonlinearity in these relationships, as expected.

Secondary aerosol formation is a more nonlinear process, which is explored by using inorganic or organic aerosol concentrations with respect to select precursors (Figs. 2e–2h). Nonlinearities in the modelled processes lead to discrepancies between HYD and FD sensitivities without tuning the FD sensitivity to capture the slope about the model state more exactly. The slopes and R^2 values of the trendline between these HYD and FD sensitivities range from 0.99 to 1.00 and 1.00 to 1.04

(Table 1), respectively. The comparisons between HYD and FD sensitivities of $s_{NO_x}^{ANO_3}$ and $s_{SO_2}^{ASO_4}$ show slight deviations from

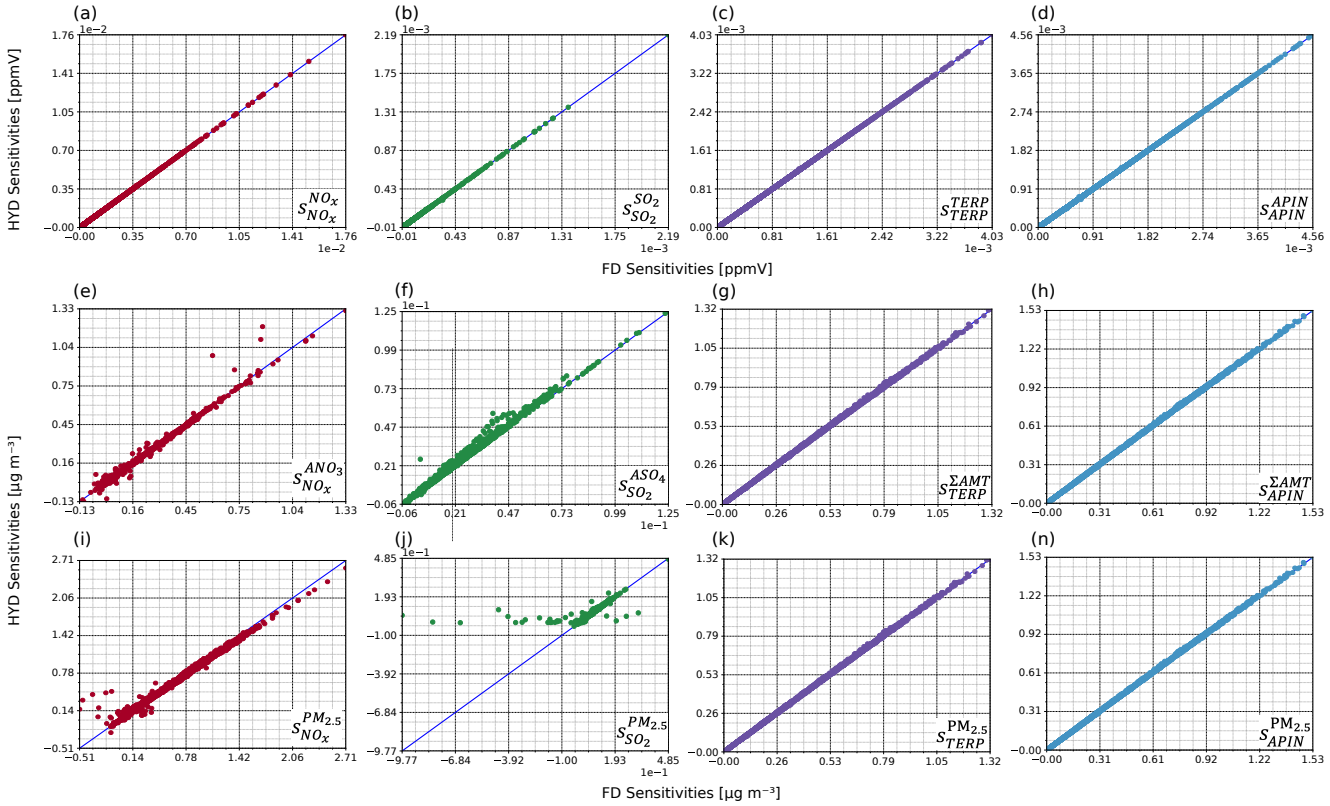

Figure 2. The comparisons of first-order sensitivities on the ground layer calculated by the hyperdual-step method (HYD sensitivities) and FDM (FD sensitivities). The sensitivities are color-coded by the perturbed emissions (i.e., NO_x, SO_2, TERP, and APIN). (a)-(d) are the gas-phase species sensitivities with respect to their emissions. APIN denotes α-pinene and TERP denotes all other monoterpene species. (e)-(h) are examples of aerosol phase products with respect to their precursors. ANO_3 denotes the total aerosol phase nitrate products. ASO_4 denotes the total aerosol sulphate products. ΣAMT denotes the total aerosol photooxidation products from monoterpene. (i)-(n) are the total $PM_{2.5}$ concentration with respect to gas-phase precursors. The sensitivities calculated are noted at the bottom-right corner of each panel with the notation pattern mentioned in Section 2.3.

the identity line, indicating some nonlinearity in their formation processes (Fig. 2e and Fig. 2f). Most points representing the HYD and FD sensitivities of total monoterpene photooxidation products to monoterpenes ($s_{TERP}^{AMTNO_3}$) and alpha-pinene ($s_{APIN}^{AMTNO_3}$) remain on the identity line (Fig. 2g and Fig. 2h).

Table 1. ~~Slope~~The slopes and R^2 ~~of~~values from the ~~comparisons~~linear regression of the first-order sensitivities of ground layer species concentrations to domain-wide perturbations~~. The plots~~ by the hyperdual-step method compared to finite difference sensitivities. The gas-phase species sensitivities with respect to their emissions are on line three, where APIN denotes α-pinene and TERP denotes all other monoterpene species. Line four includes sensitivities of aerosol phase products with respect to their precursors where ANO_3 denotes the total aerosol phase nitrate products, ASO_4 denotes the total aerosol sulphate products, and ΣAMT denotes the total aerosol photooxidation products from monoterpene. Line five includes the sensitivities of the total $PM_{2.5}$ concentration with respect to each gas-phase precursor. The visual comparison of the agreement for each relationship is shown in Figure 2.

First-order sensitivities: slope, R^2			
NO_x	SO_2	TERP	APIN
$s_{NO_x}^{NO_x}$: 1.00, 1.00	$s_{SO_2}^{SO_2}$: 1.00, 1.00	s_{TERP}^{TERP}: 1.01, 1.00	s_{APIN}^{APIN}: 1.00, 1.00
$s_{NO_x}^{ANO_3}$: 1.00, 0.99	$s_{SO_2}^{ASO_4}$: 1.04, 1.00	$s_{TERP}^{\Sigma AMT}$: 1.01, 1.00	$s_{APIN}^{\Sigma AMT}$: 1.01, 1.00
$s_{NO_x}^{PM_{2.5}}$: 0.96, 0.99	$s_{SO_2}^{PM_{2.5}}$: 0.65, 0.63	$s_{TERP}^{PM_{2.5}}$: 1.01, 1.00	$s_{APIN}^{PM_{2.5}}$: 1.03, 1.00

Regulatory models are often used to evaluate the response of total $PM_{2.5}$ to emissions changes, so the sensitivities of total $PM_{2.5}$ concentration to the four different precursor emissions are evaluated (Figs. 2i–2n). The HYD and FD sensitivities of

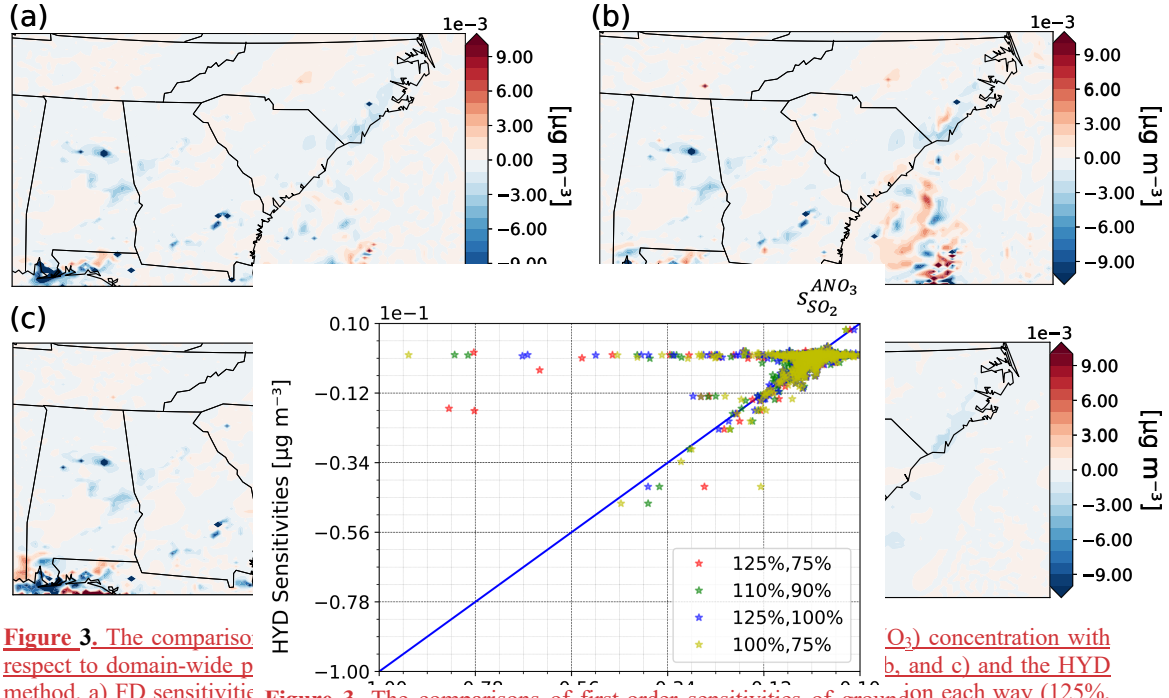

Figure 3. The compariso… respect to domain-wide p… method. a) FD sensitivitie… 75%). b) FD sensitivities … 90%). c) FD sensitivities c… d) HYD sensitivities.

…O_3) concentration with …b, and c) and the HYD …ion each way (125%, …on each way (110%, …h way (105%, 95%).

~~**Figure 3.** The comparisons of first-order sensitivities of ground-layer aerosol nitrate (ANO_3) concentration with respect to domain-wide perturbation of SO_2 emission. The HYD sensitivities are on the y-axis, and the FDM sensitivities are on the x-axis. The different perturbation sizes of FDM are color-coded. For instance, the red stars represent a central difference calculation with increased and decreased 25% of domain-wide SO_2 emission.~~

$s_{NO_x}^{PM_{2.5}}$, $s_{TERP}^{PM_{2.5}}$, and $s_{APIN}^{PM_{2.5}}$ (Fig. 2i, Fig. 2k, and Fig. 2n) agree well, with slope and R^2 values ranging from 0.96 to 1.03 and 0.99 to 1.00, respectively (Table 1). However, the agreement between HYD and FD sensitivities of $s_{SO_2}^{PM_{2.5}}$ (Fig. 2j) is much lower, with a slope of 0.65 and an R^2 value of 0.63 (Table 1). Notably, although $s_{SO_2}^{PM_{2.5}}$ is usually positive, as evidenced by most of the points on the identity line, the $s_{SO_2}^{PM_{2.5}}$ calculated by FDM sensitivities have a few negative values where the HYD and FD sensitivities disagree. Because it is highly unlikely that an ~~50~~25% increase in SO_2 emission leads to a decrease in $PM_{2.5}$ concentration, the negative FD sensitivities likely arise from truncation errors inherent to the FDM since the perturbation sizes are large (i.e., ~~50~~25% emissions perturbation). Though it is possible to refine the perturbation size to one more suitable for this particular relationship of emissions to concentration as demonstrated in the next section, this difference in one of twelve comparisons shows one of the strengths of HYD, which is the irrelevance of the perturbation size to the exactness of the resulting sensitivity.

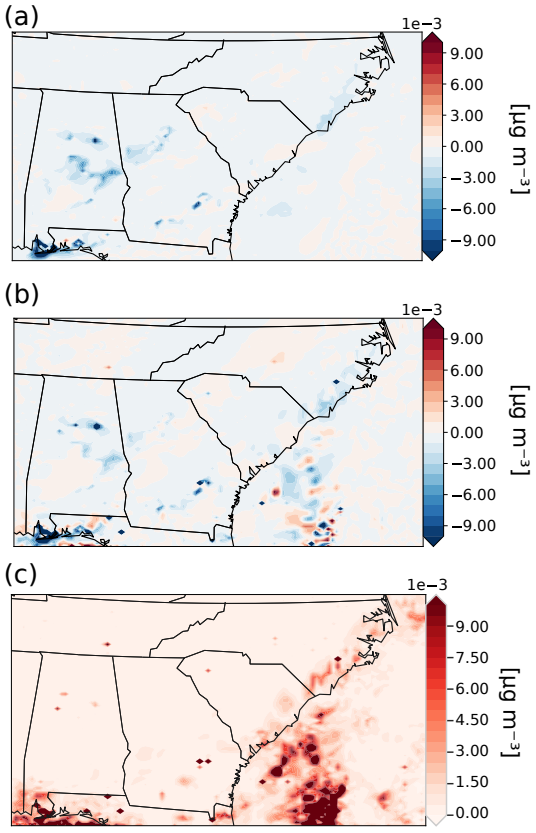

Figure 4. Comparisons of the sensitivities of aerosol phase nitrate (ANO_3) with respect to SO_2 emission calculated by HYD and FDM on a map. a) The HYD sensitivities. b) The average of the FD sensitivities with three different perturbation sizes (125%, 75%; 110%, 90%; 105%, 95%). c) The range of the FD sensitivities with four different perturbation sizes (125%, 75%; 110%, 90%; 105%, 95%).

To further illustrate the impact of nonlinear relationships between emissions and concentrations on FD sensitivities, we explored the sensitivity of ground-level aerosol nitrate to emissions of sulphur dioxide, $s_{SO_2}^{ANO_3}$, calculated with different perturbation sizes using the FDM. Our analysis revealed a low level of agreement between the FD and HYD sensitivities in the base case scenario, where the domain-wide SO_2 emission was perturbed by 125% and 75%, with a slope of 0.10 and R^2 of 0.30 (Table S1). The FD sensitivities with the base case perturbation (125 %, 75 %) and ~~three~~two other perturbation size pairs (110 %, 90 %; ~~125 %, 100 %; 100 %, 75~~105 %, 95 %) are shown in Fig. 3. The FDM sensitivities calculated with different perturbation sizes are ~~colour-coded and~~ plotted ~~against the~~ on Fig. 3a, Fig. 3b, and Fig 3c., respectively. The FDM sensitivities exhibit similar behaviour to the HYD sensitivities~~. While many points with different FDM perturbation sizes aligned closely on~~ over the ~~identity line, indicating a first-order inverse relationship between aerosol phase nitrate and SO_2 emissions, some positive sensitivities deviated from~~continents. However, the ~~identity line. These positive FD sensitivities likely resulted from numerical errors inherent to the FDM, regardless of different perturbation sizes. The lack of overlapping points~~inconsistency among the sensitivities calculated by FDM with different perturbation sizes over the ocean (Fig. 3) suggests that the FD sensitivities heavily depend on the perturbation sizes. This result ~~also shows~~demonstrates the relatively low credibility of FD sensitivities, particularly for highly nonlinear relationships where the truncation errors could be large. ~~Our findings demonstrate~~Notably, reducing perturbation sizes in the FDM did not lead to convergence with hyperdual sensitivities. This divergence may be attributed to the propagation of numerical noise from the model run to the calculated sensitivities as perturbation sizes decrease. This finding is consistent with the results in Zhang et al. (2012). Our findings highlight the importance of using other methods, including the HYD, which are not prone to truncation or cancellation errors for probing nonlinear relationships in CTMs.

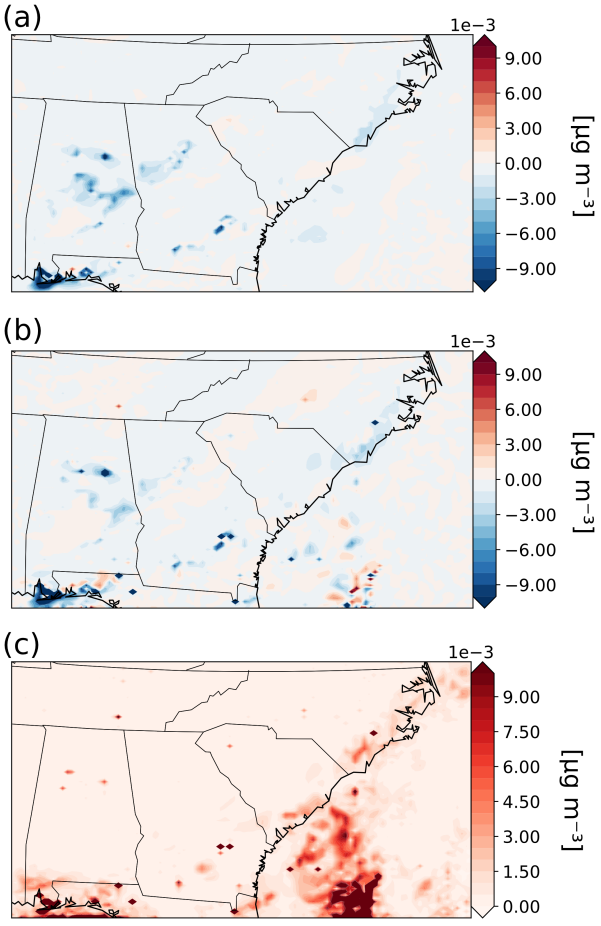

Figure 4. ~~Comparisons of the sensitivities of aerosol phase nitrate (ANO_3) with respect to SO_2 emission calculated by HYD and FDM on a map. a) The HYD sensitivities. b) The average of the FDM sensitivities with four different perturbation sizes (125%, 75%; 110%, 90%; 125%, 100%; 100%, 75%). c) The range of the FDM sensitivities with four different perturbation sizes (125%, 75%; 110%, 90%; 125%, 100%; 100%, 75%).~~

We also compared the spatial distribution of HYD sensitivities (Fig. 4a) against the average (Fig. 4b) and the range (Fig. 4c) of the FD sensitivities with ~~four~~three different perturbation sizes. ~~Maps of FDM sensitivities with four different~~

~~perturbation sizes are available in Figure S1.~~ Differences are evident between the HYD and the average FD sensitivities in central North Carolina and Tennessee as well as off the coasts of Georgia and South Carolina. The HYD predicts slightly

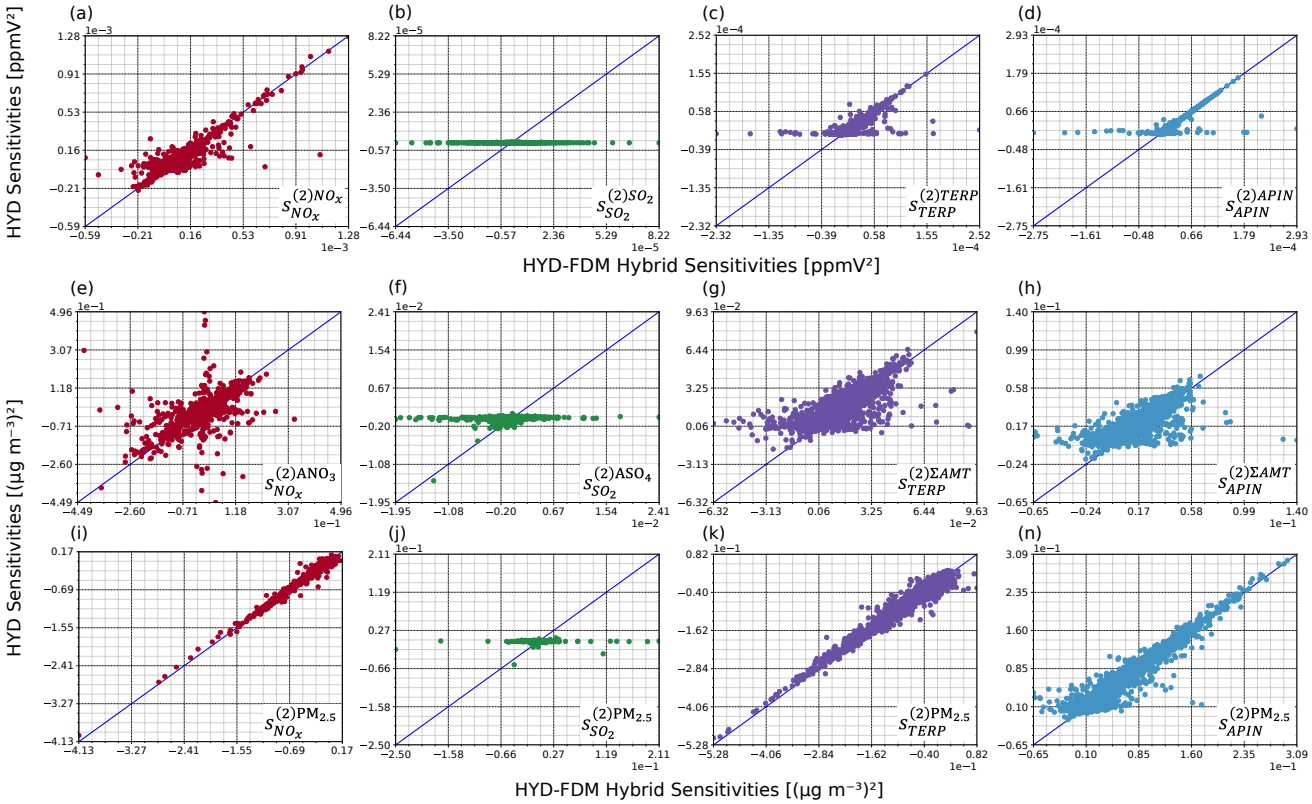

Figure 5. The comparisons of second-order sensitivities on the ground layer calculated by the hyperdual-step method (HYD sensitivities) and the hybrid HYD-FDM method (HYD-FDM sensitivities). The sensitivities are color-coded by the perturbed emissions (i.e., NO_x, SO_2, TERP, and APIN). (a)-(d) are the gas-phase species sensitivities with respect to their emissions. APIN denotes α-pinene and TERP denotes all other monoterpene species. (e)-(h) are examples of aerosol phase products with respect to their precursors. ANO_3 denotes the total aerosol phase nitrate products. ASO_4 denotes the total aerosol sulphate products. ΣAMT denotes the total aerosol photooxidation products from monoterpene. (i)-(n) are the total $PM_{2.5}$ concentration with respect to gas-phase precursors. The sensitivities calculated are noted at the bottom-right corner of each panel with the notation pattern mentioned in Section2.3.

negative sensitivities in North Carolina and Tennessee while the FDM predicts slightly positive values. The average FDM sensitivities off the coast of Georgia and South Carolina were noisy, with alternating positive and negative sensitivities, while the HYD sensitivities were much less noisy. In addition, the range of FDM sensitivities with different perturbation sizes was large (Fig. 4c), especially off the coast Georgia and South Carolina. The results shown in Fig. 4b and Fig. 4c illustrate the dependence of FDM sensitivities on perturbation sizes especially for highly nonlinear relationships.

We also compared the second-order HYD sensitivities with those calculated from the hybrid HYD-FDM method (hybrid second-order sensitivities) described in Section 2.3 using one-to-one plots with identity lines for each panel (Fig. 4)

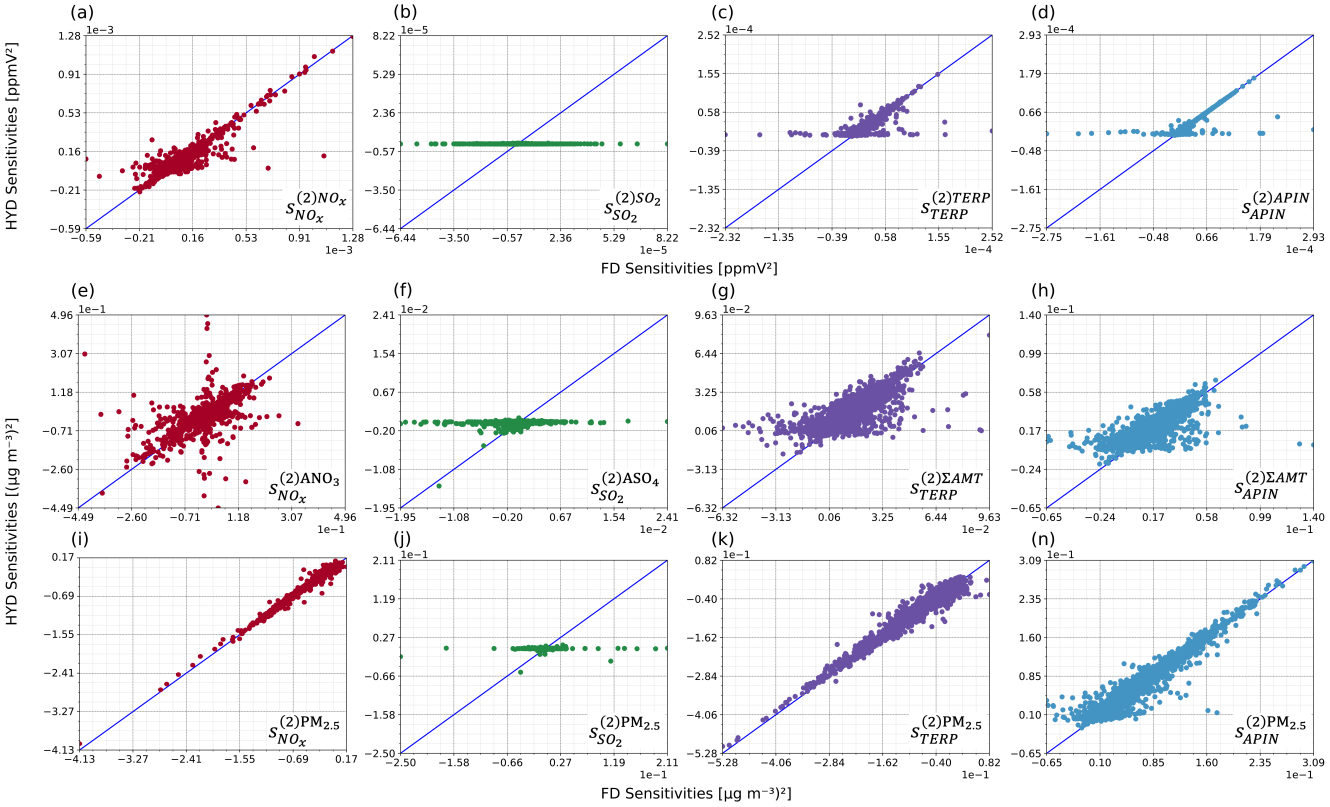

~~**Figure 5.** The comparisons of second-order sensitivities on the ground layer calculated by the hyperdual-step method (HYD sensitivities) and FDM (FD sensitivities). The sensitivities are color-coded by the perturbed emissions (i.e., NO_x, SO_2, TERP, and APIN). (a)-(d) are the gas-phase species sensitivities with respect to their emissions. APIN denotes α-pinene and TERP denotes all other monoterpene species. (e)-(h) are examples of aerosol phase products with respect to their precursors. ANO_3 denotes the total aerosol phase nitrate products. ASO_4 denotes the total aerosol sulphate products. ΣAMT denotes the total aerosol photooxidation products from monoterpene. (i)-(n) are the total $PM_{2.5}$ concentration with respect to gas-phase precursors. The sensitivities calculated are noted at the bottom-right corner of each panel with the notation pattern mentioned in section 2.3~~

along with the slope and R^2 values (Table 2). Additional slopes and R^2 values for second-order sensitivities can be found in Table S1 and Table S2. Overall, the agreement between HYD and the hybrid second-order sensitivities is good, except for those to SO_2 emissions. This result can be attributed to the numerical errors in the first-order sensitivities to SO_2, as illustrated in Fig. 2j and Fig. 3. Computing second-order sensitivities with the hybrid method, which includes FDM, is expected to add numerical noise. Except for $s^{(2)SO_2}_{SO_2}$, the gas phase species concentrations to their emissions still exhibit good agreement, with slopes and R^2 values ranging from 0.84 to 0.85 and 0.84 to 0.86, respectively (Table 2). The hybrid second-order sensitivities are sometimes large, while HYD predicts close to zero sensitivities. This result is especially evident in $s^{(2)TERP}_{TERP}$ (Fig. 5c) and $s^{(2)APIN}_{APIN}$ (Fig. 5d). This spread in the hybrid sensitivities likely originates from the FDM step, which is subject to numerical

errors. Figures 5e–5h show the HYD and HYD-FDM sensitivities of aerosol phase product concentrations to the precursor emissions for this modelling period. Except for $s_{SO_2}^{ASO_4}$, the slope and R^2 values range from 0.61 to 0.82 and 0.38 to 0.71, respectively (Table 2). The degree of agreement for $s_{NO_x}^{ANO_3}$ is slightly lower than those for $s_{TERP}^{\Sigma AMT}$ and $s_{APIN}^{\Sigma AMT}$, indicating more nonlinearity in the formation process from NO_x to aerosol nitrate. The second-order sensitivities of total $PM_{2.5}$ to different precursors demonstrate excellent agreement with slope and R^2 values ranging from 0.95 to 0.99 and 0.96 to 0.99 (Table 2), again excluding the one to SO_2. The second-order sensitivities of $PM_{2.5}$ to NO_x and α-pinene are primarily negative, while positive to monoterpenes. These findings have important implications for the formation process of $PM_{2.5}$ from monoterpenes and α-pinene, which will be discussed in detail in the next section.

Table 2. ~~Slope~~The slopes and R^2 ~~of~~values from the ~~comparisons~~linear regression of the second-order sensitivities of ground layer species concentrations to domain-wide perturbations ~~of selected~~by the hyperdual-step method compared to finite difference sensitivities. The gas-phase species sensitivities with respect to their emissions~~. The plots~~ are on line three, where APIN denotes α-pinene and TERP denotes all other monoterpene species. Line four includes sensitivities of aerosol phase products with respect to their precursors where ANO_3 denotes the total aerosol phase nitrate products, ASO_4 denotes the total aerosol sulphate products, and ΣAMT denotes the total aerosol photooxidation products from monoterpene. Line five includes the sensitivities of the total $PM_{2.5}$ concentration with respect to each gas-phase precursor. The visual comparison of the agreement for each relationship is shown in Figure 5.

Second-order sensitivities: slope, R^2			
NO_x	SO_2	TERP	APIN
$s_{NO_x}^{NO_x}$: 0.84, 0.84	$s_{SO_2}^{SO_2}$: 0.00, 0.00	s_{TERP}^{TERP}: 0.84, 0.84	s_{APIN}^{APIN}: 0.85, 0.86
$s_{NO_x}^{ANO_3}$: 0.61, 0.38	$s_{SO_2}^{ASO_4}$: 0.04, 0.06	$s_{TERP}^{\Sigma AMT}$: 0.79, 0.71	$s_{APIN}^{\Sigma AMT}$: 0.82, 0.71
$s_{NO_x}^{PM_{2.5}}$: 0.98, 0.99	$s_{SO_2}^{PM_{2.5}}$: 0.01, 0.01	$s_{TERP}^{PM_{2.5}}$: 0.95, 0.98	$s_{APIN}^{PM_{2.5}}$: 0.99, 0.96

3.2 Sensitivities of biogenic aerosol formation in the southeast US computed by CMAQ-hyd

In this section, the first- and second-order sensitivities of several biogenic aerosols to both anthropogenic and biogenic aerosol precursors in the southeast US are explored. The importance of calculating second-order sensitivities is demonstrated through the spatial distributions of the first- and second-order sensitivities of total aerosol phase monoterpene photooxidation product (ΣAMT) and $PM_{2.5}$ concentrations (Fig. 6). The first-order sensitivities (Figs. 6a–6d) are predominantly positive, indicating that an increase in either TERP or APIN emissions will lead to an increase in ground-layer ΣAMT and $PM_{2.5}$

concentrations. While $s_{TERP}^{\Sigma AMT}$ (Fig. 6a) and $s_{APIN}^{\Sigma AMT}$ (Fig. 6b) have similar values, $s_{TERP}^{PM_{2.5}}$ (Fig. 6c) is slightly larger than $s_{APIN}^{PM_{2.5}}$ (Fig. 6d) due to the formation of other species, such as aerosol phase monoterpene nitrate products ($AMTNO_3$).

The second-order sensitivities (Fig. 6e–6h) provide additional information about how ΣAMT and $PM_{2.5}$ concentrations respond to changes in APIN and TERP emissions. The $s_{TERP}^{(2)\Sigma AMT}$ (Fig. 6e) and $s_{APIN}^{(2)\Sigma AMT}$ (Fig. 6f) are generally positive, indicating the concentration of ΣAMT to monoterpene and α-pinene emissions is convex. An increase in either monoterpene or α-pinene emissions will lead to an increase in $s_{TERP}^{\Sigma AMT}$ and $s_{APIN}^{\Sigma AMT}$. If we only consider first-order sensitivities, the effect of changes in TERP or APIN emissions on ΣAMT concentrations would be underestimated. On the other hand, the $s_{TERP}^{(2)PM_{2.5}}$ (Fig. 6g) is mostly ~~positive~~negative, while $s_{APIN}^{(2)PM_{2,5}}$ (Fig. 6h) is mostly ~~negative~~positive. The distinct behaviour of second-order sensitivities of $PM_{2.5}$ concentration to either TERP or APIN emissions exemplify the importance of considering second-order sensitivities for these nonlinear formation processes. Only considering the first-order sensitivities often leads to overestimating or underestimating the effects. The accurate second-order sensitivity information can help researchers understand the relationships of concentration to emissions more thoroughly and develop emission control strategies for specific aerosol precursor emissions.

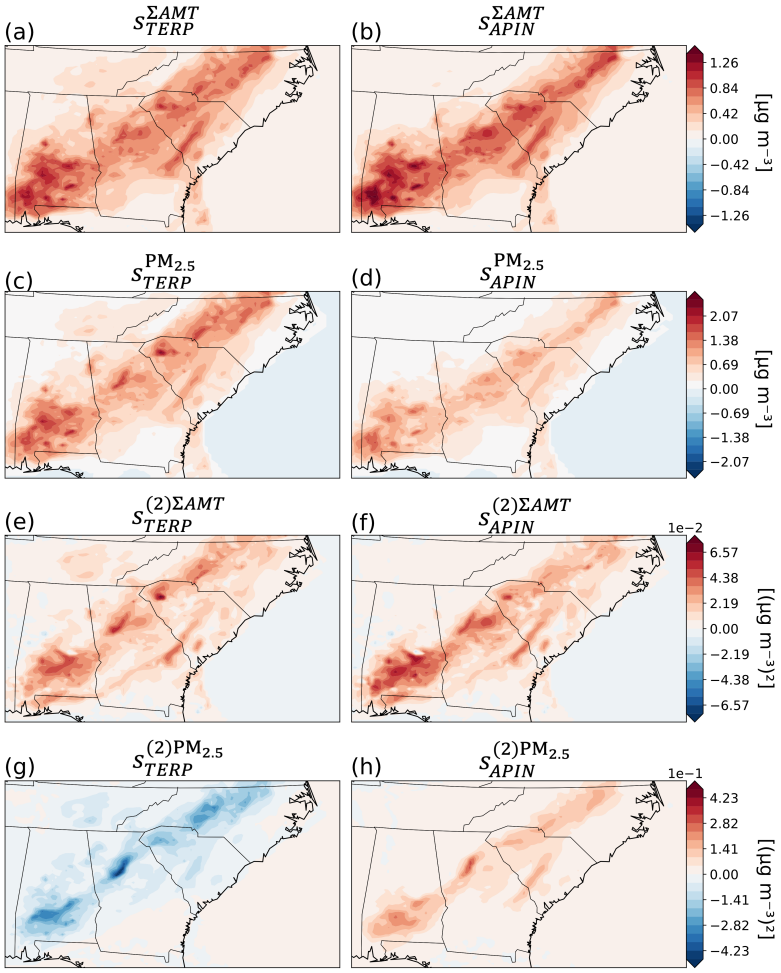

Figure 6. The first- and second-order sensitivities of total aerosol monoterpene photooxidation products (ΣAMT) and $PM_{2.5}$ with respect to monoterpenes (TERP) and alpha-pinene (APIN) emissions plotted on a map. (a)-(d) are the first-order sensitivities and (e)-(h) are the second-order sensitivities.

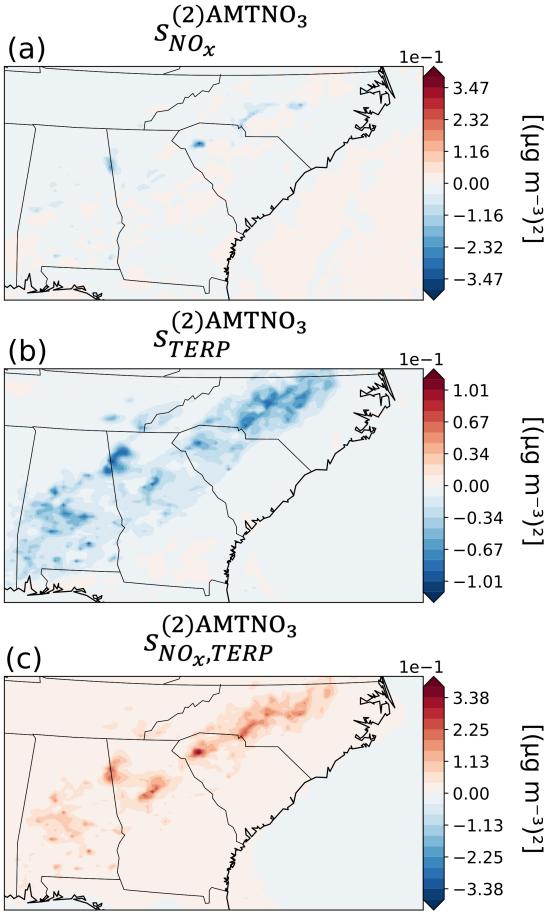

Figure 7. The second-order sensitivities and cross-sensitivities of aerosol phase monoterpene nitrate products ($AMTNO_3$) with respect to NO_x and monoterpenes (TERP) emissions plotted on a map. (a). second-order sensitivities of $AMTNO_3$ with respect to NOx. (b). second-order sensitivities of $AMTNO_3$ with respect to TERP. (c) cross-sensitivities of $AMTNO_3$ with respect to NO_x and TERP

We used the formation of aerosol monoterpene nitrate, $AMTNO_3$, as an example of the importance of computing the cross-sensitivity, especially for complex anthropogenic-biogenic aerosol formation processes. The formation of $AMTNO_3$ is influenced primarily by two precursors: NO_x and monoterpenes. NO_x is primarily emitted anthropogenically while monoterpenes primarily originate from biogenic sources. The first- and second-order sensitivities of $AMTNO_3$ to NO_x or TERP can help researchers and environmental decision makers estimate the nonlinear effects of emissions changes on concentrations of secondary pollutants. The cross-sensitivity of $AMTNO_3$ with respect to both NO_x and TERP emissions, $s_{NO_x,TERP}^{(2)\mathrm{AMTNO_3}}$, is a valuable tool for answering complex research questions. For instance, researchers can use $s_{NO_x,TERP}^{(2)\mathrm{AMTNO_3}}$ to predict how an increase in monoterpene emissions would affect the first-order sensitivities of $AMTNO_3$ to NO_x. Since biogenic emissions of monoterpenes are temperature-dependent, understanding how anthropogenic emissions of NO_x will affect $AMTNO_3$ formation with changing terpene emissions in future scenarios is crucial for designing effective air pollution control strategies. Computing the cross-sensitivity is especially challenging with traditional methods since determining the proper perturbation for two species using FDM is even harder than calculating second-order sensitivities with FDM. The distinct values of $s_{NO_x}^{(2)AMTNO_3}$, $s_{TERP}^{(2)AMTNO_3}$, and $s_{NO_x,TERP}^{(2)\mathrm{AMTNO_3}}$ demonstrate the value of the HYD method (Fig. 7). The spatial distributions of $s_{NO_x}^{AMTNO_3}$ and $s_{TERP}^{AMTNO_3}$ are included in Fig. ~~S2~~S1. Overall, the second-order sensitivities are negative over land in the southeast US. The $s_{NO_x}^{(2)AMTNO_3}$ is generally smaller than $s_{TERP}^{(2)AMTNO_3}$, indicating the relationship between $AMTNO_3$ and TERP emissions is more nonlinear than that between $AMTNO_3$ and NO_x. The cross-sensitivities $s_{NO_x,TERP}^{(2)\mathrm{AMTNO_3}}$ are mostly positive over the southeast US. Based on the cross-sensitivity results, we can conclude that an increase in TERP emission will make the first-order sensitivity of $AMTNO_3$ to NO_x larger. A warmer climate in the future would likely increase the impact of anthropogenic NO_x on $AMTNO_3$ concentration in the atmosphere. This kind of information

is invaluable for researchers and environmental decisionmakers to evaluate complex secondary organic aerosol formation with multiple anthropogenic and biogenic precursors.

3.3 Computational cost of the CMAQ-hyd

The practical application of any sensitivity analysis in CTMs depends heavily upon its computational cost. Previous works using operator overloading approaches resulted in high computational costs due to additional mathematical operations, making this approach computationally unfavourable compared to other existing methods. For instance, the implementation of CVM in GEOS-CHEM ~~is 4.5 times higher than the regular~~results in a 4.5-fold increase in computational overhead when compared to the standard model ~~(Constantin and Barrett, 2014)~~(Constantin and Barrett, 2014). To evaluate the computational

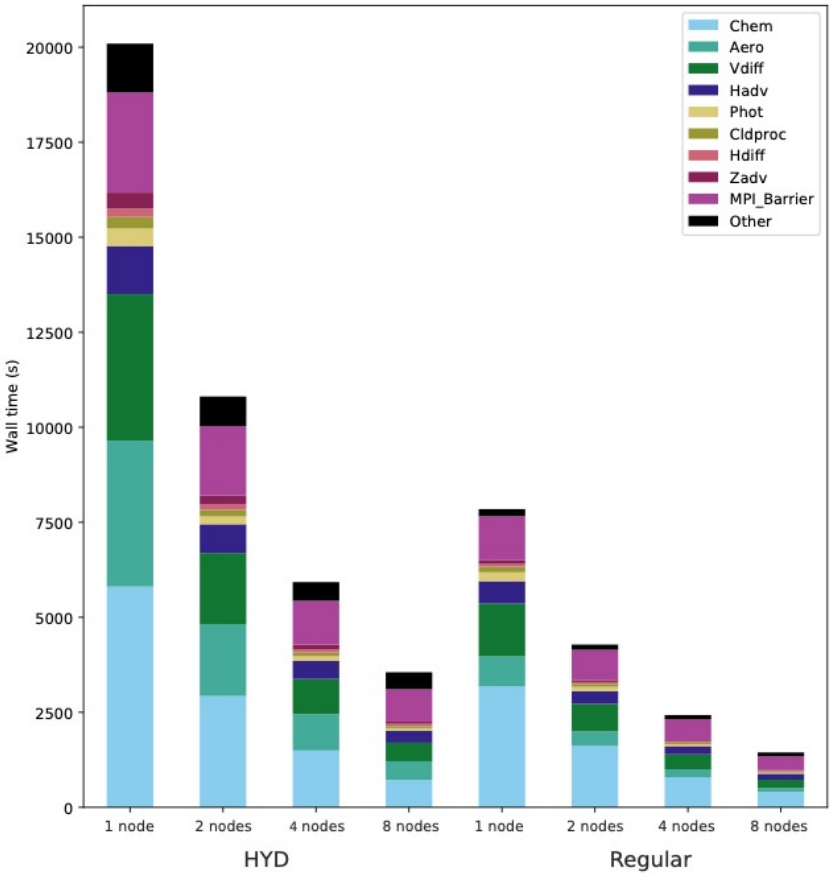

efficiency of CMAQ-hyd, we compared it with a standard CMAQ model using different computational resources on a

Figure 8. Computational cost of CMAQ-hyd and standard CMAQ separated by different modules. The CMAQ-hyd and standard CMAQ simulations with different number of 1, 2, 4, and 8 nodes and are shown on the x-axis. The wall time is shown on the y-axis.

supercomputing cluster. The total wall time ~~of~~with different numbers of computational nodes used for an identical run of the original CMAQ model and CMAQ-hyd ~~ are shown for the when using different numbers of nodes~~ is displayed (Fig. 8). The CMAQ-hyd and ~~regular~~standard CMAQ runs were performed with 1, 2, 4, and 8 nodes on the supercomputing cluster. The configuration of computing resources is detailed in Section 4 of the SI. Profiling of the model was completed at the level of the scientific modules, special subroutines, or other important components of CMAQ. The scientific processes are Chem (gas-phase chemistry), Aero (aerosol dynamics and thermodynamics), Vdiff (vertical diffusion), Hadv (Horizontal advection), Phot (Photolysis), Cldproc (cloud processes), Hdiff (horizontal diffusion), and Zadv (vertical advection). The MPI_Barrier is a special subroutine used for synchronising processes among parallel processors after vertical diffusion and before all three other transport processes. Other processes necessary for CMAQ, including the I/O processes, are included in the "Other" category. The details of the high-performance computing cluster used can be found in the SI.

With the same computing resources, the total computation time of the CMAQ-hyd is approximately 2.5 (2.44–2.56) times longer. Despite the additional computation burden, CMAQ-hyd remains computationally competitive with the traditional FDM when calculating derivatives. One run of CMAQ-hyd generates the same amount of first- and second-order sensitivity information as at least three runs of ~~regular~~standard CMAQ. The relatively low computational cost of CMAQ-hyd, compared

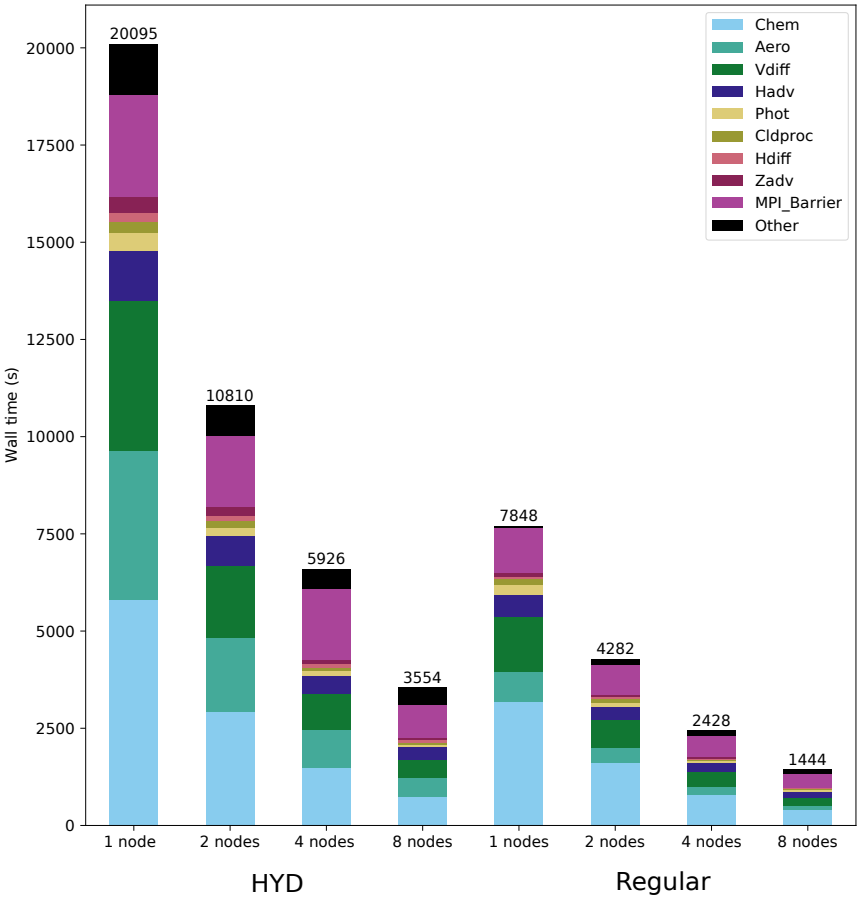

~~**Figure 8.** Computational cost of CMAQ-hyd separated by different modules. The CMAQ-hyd and regular CMAQ simulations with different number of 1, 2, 4, and 8 nodes and are shown on the x-axis. The wall time is shown on the y-axis.~~

to the previous operator overloading approach, may be due to the selective modification of the source code. In contrast to GEOS-CHEM CVM ~~(Constantin and Barrett, 2014)~~(Constantin and Barrett, 2014), only parts of the model that involve calculating the main species concentration array use hyperdual calculations. ~~The computation time of CMAQ-hyd also scales well with increases in computational resources, similar to the original CMAQ. The overall memory overhead of the CMAQ-hyd is approximately 25 GB for this simulation. A parallel input/output (I/O) approach may be applied to reduce the possibility of potential memory overflow in processor 0 (Wong et al., 2015). The computation time of each module is detailed in Table S3.~~

The computational time of scientific modules in CMAQ-hyd generally scales well with increases in computational resources, similar to the standard CMAQ. Chem, Aero, and Vdiff are the most computationally expensive modules in both CMAQ and CMAQ-hyd. The relative computational cost of Aero is higher in the CMAQ-hyd than in the ~~regular CMAQ.~~standard CMAQ. The ratio of computational time of Chem to Aero is 1.53 (1.49–1.56) for the CMAQ-hyd runs and 3.98 (3.85–4.19) for the standard CMAQ runs (Fig. 8). Future work can potentially reduce the computational cost by ignoring sensitivity propagations during the iterative root-finding process in select subroutines, since only the output concentrations from these subroutines are used in the later part of the model. This is also a significant advantage of any operator overloading-based approach (Fike and Alonso, 2011). The computational time of each module is detailed in Table S3, and the full relative percentage of computational time of each module of eight runs is shown in Figure S2.

The MPI_Barrier function also scales well with an increasing number of processors. To a certain point, subdividing the domain further reduces the variability of the time required for science processes to be completed across different nodes, resulting in a reduction of the amount of time the program spends waiting for all processes to be synchronized. One important thing to note here is that the scaling of MPI_barrier is dependent on the ratio of the number of nodes to the number of grid cells. A demonstration of the subdivision the modelling domain by processors is shown in Fig. S3.

The I/O process of newly added first- and second-order sensitivity output files increases the computational cost; however, the I/O of species concentration files has a much lower computational cost than other ~~computing~~ modules in CMAQ for this specific scenario. The I/O processes of CMAQ-hyd and CMAQ take 193 (181–206) seconds and 52 (47–56) seconds, respectively. The I/O process in CMAQ-hyd takes approximately 3.7 times longer on average than that in the standard CMAQ. The overall memory overhead of the CMAQ-hyd is approximately 25 GB for this simulation. A parallel input/output (I/O) approach may be applied to reduce the possibility of potential memory overflow in processor 0

(Wong et al., 2015).

4 Conclusion

We demonstrate the implementation of the hyperdual-step method in CMAQ version 5.3.2 to formulate CMAQ-hyd. This novel model retains the majority of CMAQ code with slight modifications in declarations of selected variables and the addition of sensitivity computation modules. The novel model can be applied to compute exact first-order, second-order, and cross-sensitivities of pollutant concentrations efficiently and accurately to precursor emissions with a single model run. Compared with traditional sensitivity analysis methods, CMAQ-hyd is computationally competitive with conventional methods and easier to maintain than other existing advanced methods (DDM and adjoint). The development process of CMAQ-hyd is also more straightforward than that of other advanced methods since all that is needed is to change the type of newly declared variables to hyperdual.

We developed and validated the hyperdual-step module "HDMod", which ~~involves~~is limited to analytically verifiable mathematical operations of hyperdual numbers. This module can also be applied to other numerical models where first- and second-order sensitivities are of interest. We further ~~validated~~evaluated the development of CMAQ-hyd against the FDM and FDM-HYD hybrid method to ensure the correctness of the implementation. During the ~~validation~~evaluation process, CMAQ-hyd demonstrated the ability to compute sensitivities free from ~~numerical noise, different from~~truncation and subtractive cancellation errors, unlike those calculated by the FDM. HDMod can potentially be applied to other numerical models written in Fortran to produce first- and second-order sensitivities.

The computation of second-order sensitivities is crucial for researchers and environmental decision-makers to decide the priority and extent of controls of specific types of emissions to reduce atmospheric pollutant concentrations. For instance, the second-order sensitivity of $PM_{2.5}$ concentration to monoterpenes and α-pinene provided additional information about relationships of emissions to concentrations in CMAQ. With the additional second-order sensitivity information, the curvature of the concentration responses to emissions changes improves the estimate of how a specific pollutant concentration would respond to changes in emissions. The simplicity of computing cross-sensitivities with CMAQ-hyd is another advantage of this augmented model. Cross-sensitivities are especially useful in nonlinear processes with two precursors. The synergistic effect of anthropogenic and biogenic emission on aerosol concentrations (e.g., NO_x and monoterpene on $AMTNO_3$) is essential for researchers to predict the dynamics between two potential pollutants and for environmental decision-makers to propose policy implementations under different climate scenarios in the future.

Although CMAQ-hyd remains computationally competitive with the traditional finite-difference method, it is still computationally intensive and has a memory overhead. We plan to implement optimisations for iterative processes in CMAQ and apply the parallel I/O approach to reduce the memory overhead on the compute node where all the information is gathered. The implementation of checkpointing of sensitivities after specific subroutines is also a potential advantage of CMAQ-hyd and will provide valuable information of how each module or even each line of the model affects the sensitivities, akin to a process analysis approach. This checkpointing feature cannot be easily implemented with other methods such as FDM, DDM, and the adjoint method.

In conclusion, we have developed and evaluated CMAQ-hyd, a novel augmented model to compute first-order, second-order, and cross-sensitivities free from ~~numerical noise~~subtractive cancellation and truncation errors in CMAQ. Our successful implementation also provides an example of the hyperdual-step method that may be applicable for other CTMs where sensitivities are helpful.

Code and Data Availability. CMAQv5.3.2 is available at https://github.com/USEPA/CMAQ/tree/5.3.2 and is archived at https://doi.org/10.5281/zenodo.4081737 ~~(U.S. Environmental Protection Agency, 2020)~~(U.S. Environmental Protection Agency, 2020). The CMAQ-hyd model is archived at https://doi.org/10.5281/zenodo.10119026~~7938726~~ (Liu, 2023). Both the

CMAQv5.3.2 and the CMAQ-hyd models are under MIT licenses. The input data for the simulation experiments is available at https://doi.org/10.15139/S3/IQVABD ~~(U.S. Environmental Protection Agency, 2019)~~(U.S. Environmental Protection Agency, 2019).

Author contribution. JL developed the model code and performed the simulations with ~~the~~ help from SC. EC helped develop and test the "HDMod" library. JL prepared the manuscript with ~~the help~~ guidance from SC.

Competing Interests. The authors declare that they have no conflict of interest.

Acknowledgements. The work is supported by National Science Foundation CAREER Award Grant No. 1944669 to SC. The authors would also like to thank Dr. Ryan P. Russell for kindly providing the testing framework of multicomplex numbers, which inspired the development of the testing framework for hyperdual numbers.

References

Berman, B., Capps, S. L., Sauvageau, I., Gao, E., Eastham, S. D., and Russell, R. P.: ISORROPIA-MCX: Enabling Sensitivity Analysis With Multicomplex Variables in the Aerosol Thermodynamic Model, ISORROPIA, Earth and Space Science, 10, e2022EA002729, https://doi.org/10.1029/2022EA002729, 2023.

Boole, G.: A Treatise on the Calculus of Finite Difference, 2nd Ed Dover1960.

Byun, D. and Schere, K. L.: Review of the Governing Equations, Computational Algorithms, and Other Components of the Models-3 Community Multiscale Air Quality (CMAQ) Modeling System, Applied Mechanics Reviews, 59, 51-77, 10.1115/1.2128636, 2006.

Capaldo, K. P., Pilinis, C., and Pandis, S. N.: A computationally efficient hybrid approach for dynamic gas/aerosol transfer in air quality models, Atmospheric Environment, 34, 3617-3627, https://doi.org/10.1016/S1352-2310(00)00092-3, 2000.

Che, W., Zheng, J., Wang, S., Zhong, L., and Lau, A.: Assessment of motor vehicle emission control policies using Model-3/CMAQ model for the Pearl River Delta region, China, Atmospheric Environment, 45, 1740-1751, https://doi.org/10.1016/j.atmosenv.2010.12.050, 2011.

Chemel, C., Fisher, B. E. A., Kong, X., Francis, X. V., Sokhi, R. S., Good, N., Collins, W. J., and Folberth, G. A.: Application of chemical transport model CMAQ to policy decisions regarding PM2.5 in the UK, Atmospheric Environment, 82, 410-417, 10.1016/j.atmosenv.2013.10.001, 2014.

Cohan, D. S. and Napelenok, S. L.: Air Quality Response Modeling for Decision Support, Atmosphere, 2, 407-425, 10.3390/atmos2030407, 2011.

Constantin, B. V. and Barrett, S. R. H.: Application of the complex step method to chemistry-transport modeling, Atmospheric Environment, 99, 457-465, https://doi.org/10.1016/j.atmosenv.2014.10.017, 2014.

Dunker, A. M.: Efficient calculation of sensitivity coefficients for complex atmospheric models, Atmospheric Environment (1967), 15, 1155-1161, 10.1016/0004-6981(81)90305-x, 1981.

Fike, J. and Alonso, J.: The Development of Hyper-Dual Numbers for Exact Second-Derivative Calculations, 49th AIAA Aerospace Sciences Meeting including the New Horizons Forum and Aerospace Exposition, 2011-01-04, 10.2514/6.2011-886,

Fornberg, B.: Numerical Differentiation of Analytic Functions, ACM Trans. Math. Softw., 7, 512-526, 10.1145/355972.355979, 1981.

Fountoukis, C. and Nenes, A.: ISORROPIA II: a computationally efficient thermodynamic equilibrium model for K⁺–Ca²⁺–Mg²⁺–NH₄&amp, Atmospheric Chemistry and Physics, 7, 4639-4659, 10.5194/acp-7-4639-2007, 2007.

Fuller, R., Landrigan, P. J., Balakrishnan, K., Bathan, G., Bose-O'Reilly, S., Brauer, M., Caravanos, J., Chiles, T., Cohen, A., Corra, L., Cropper, M., Ferraro, G., Hanna, J., Hanrahan, D., Hu, H., Hunter, D., Janata, G., Kupka, R., Lanphear, B., Lichtveld, M., Martin, K., Mustapha, A., Sanchez-Triana, E., Sandilya, K., Schaefli, L., Shaw, J., Seddon, J., Suk, W., Téllez-Rojo, M. M., and Yan, C.: Pollution and health: a progress update, The Lancet Planetary Health, 6, e535-e547, 10.1016/s2542-5196(22)00090-0, 2022.

Hakami, A.: Nonlinearity in atmospheric response: A direct sensitivity analysis approach, Journal of Geophysical Research, 109, 10.1029/2003jd004502, 2004.

Hakami, A., Odman, M. T., and Russell, A. G.: High-order, direct sensitivity analysis of multidimensional air quality models, Environ Sci Technol, 37, 2442-2452, 10.1021/es020677h, 2003.

Hennigan, C. J., Izumi, J., Sullivan, A. P., Weber, R. J., and Nenes, A.: A critical evaluation of proxy methods used to estimate the acidity of atmospheric particles, Atmospheric Chemistry and Physics, 15, 2775-2790, 10.5194/acp-15-2775-2015, 2015.

Kwok, R. H. F., Napelenok, S. L., and Baker, K. R.: Implementation and evaluation of PM2.5 source contribution analysis in a photochemical model, Atmospheric Environment, 80, 398-407, https://doi.org/10.1016/j.atmosenv.2013.08.017, 2013.

Kwok, R. H. F., Baker, K. R., Napelenok, S. L., and Tonnesen, G. S.: Photochemical grid model implementation and application of VOC, NO_x, and O₃ source apportionment, Geoscientific Model Development, 8, 99-114, 10.5194/gmd-8-99-2015, 2015.

Lantoine, G., Russell, R. P., and Dargent, T.: Using Multicomplex Variables for Automatic Computation of High-Order Derivatives, ACM Trans. Math. Softw., 38, 1-21, 10.1145/2168773.2168774, 2012.

Li, Q., Borge, R., Sarwar, G., De La Paz, D., Gantt, B., Domingo, J., Cuevas, C. A., and Saiz-Lopez, A.: Impact of halogen chemistry on summertime air quality in coastal and continental Europe: application of the CMAQ model and implications for regulation, Atmospheric Chemistry and Physics, 19, 15321-15337, 10.5194/acp-19-15321-2019, 2019.

Liu, J. C., Eric, Capps, Shannon: CMAQv5.3.2-hyd (5.3.2-hyd1.0.1), Zenodo [code], 10.5281/zenodo.10119026, 2023.

Liu, X.-H., Zhang, Y., Cheng, S.-H., Xing, J., Zhang, Q., Streets, D. G., Jang, C., Wang, W.-X., and Hao, J.-M.: Understanding of regional air pollution over China using CMAQ, part I performance evaluation and seasonal variation, Atmospheric Environment, 44, 2415-2426, https://doi.org/10.1016/j.atmosenv.2010.03.035, 2010.

Luecken, D. J., Yarwood, G., and Hutzell, W. T.: Multipollutant modeling of ozone, reactive nitrogen and HAPs across the continental US with CMAQ-CB6, Atmospheric Environment, 201, 62-72, https://doi.org/10.1016/j.atmosenv.2018.11.060, 2019.

Lyness, J. and Moler, C.: Numerical Differentiation of Analytic Functions, SIAM Journal on Numerical Analysis, 4, 202-210, 10.1137/0704019, 1967.

Mebust, M. R., Eder, B. K., Binkowski, F. S., and Roselle, S. J.: Models-3 Community Multiscale Air Quality (CMAQ) model aerosol component 2. Model evaluation, Journal of Geophysical Research: Atmospheres, 108, 10.1029/2001jd001410, 2003.

Murray, C. J. L. and Aravkin, A. Y. and Zheng, P. and Abbafati, C. and Abbas, K. M. and Abbasi-Kangevari, M. and Abd-Allah, F. and Abdelalim, A. and Abdollahi, M. and Abdollahpour, I. and Abegaz, K. H. and Abolhassani, H. and Aboyans, V. and Abreu, L. G. and Abrigo, M. R. M. and Abualhasan, A. and Abu-Raddad, L. J. and Abushouk, A. I. and Adabi, M. and Adekanmbi, V. and Adeoye, A. M. and Adetokunboh, O. O. and Adham, D. and Advani, S. M. and Agarwal, G. and Aghamir, S. M. K. and Agrawal, A. and Ahmad, T. and Ahmadi, K. and Ahmadi, M. and Ahmadieh, H. and Ahmed, M. B. and Akalu, T. Y. and Akinyemi, R. O. and Akinyemiju, T. and Akombi, B. and Akunna, C. J. and Alahdab, F. and Al-Aly, Z. and Alam, K. and Alam, S. and Alam, T. and Alanezi, F. M. and Alanzi, T. M. and Alemu, B. W. and Alhabib, K. F. and Ali, M. and Ali, S. and Alicandro, G. and Alinia, C. and Alipour, V. and Alizade, H. and Aljunid, S. M. and Alla, F. and Allebeck, P. and Almasi-Hashiani, A. and Al-Mekhlafi, H. M. and Alonso, J. and Altirkawi, K. A. and Amini-Rarani, M. and Amiri, F. and Amugsi, D. A. and Ancuceanu, R. and Anderlini, D. and Anderson, J. A. and Andrei, C. L. and Andrei, T. and Angus, C. and Anjomshoa, M. and Ansari, F. and Ansari-Moghaddam, A. and Antonazzo, I. C. and Antonio, C. A. T. and Antony, C. M. and Antriyandarti, E. and Anvari, D. and Anwer, R. and Appiah, S. C. Y. and Arabloo, J. and Arab-Zozani, M. and Ariani, F. and Armoon, B. and Ärnlöv, J. and Arzani, A. and Asadi-Aliabadi, M. and Asadi-Pooya, A. A. and Ashbaugh, C. and Assmus, M. and Atafar, Z. and Atnafu, D. D. and Atout, M. M. D. W. and Ausloos, F. and Ausloos, M. and Ayala Quintanilla, B. P. and Ayano, G. and Ayanore, M. A. and Azari, S. and Azarian, G. and Azene, Z. N. and Badawi, A. and Badiye, A. D. and Bahrami, M. A. and Bakhshaei, M. H. and Bakhtiari, A. and Bakkannavar, S. M. and Baldasseroni, A. and Ball, K. and Ballew, S. H. and Balzi, D. and Banach, M. and Banerjee, S. K. and Bante, A. B. and Baraki, A. G. and Barker-Collo, S. L. and Bärnighausen, T. W. and Barrero, L. H. and Barthelemy, C. M. and Barua, L. and Basu, S. and Baune, B. T. and Bayati, M. and Becker, J. S. and Bedi, N. and Beghi, E. and Béjot, Y. and Bell, M. L. and Bennitt, F. B. and Bensenor, I. M. and Berhe, K. and Berman, A. E. and Bhagavathula, A. S. and Bhageerathy, R. and Bhala, N. and Bhandari, D. and Bhattacharyya, K. and Bhutta, Z. A. and Bijani, A. and Bikbov, B. and Bin Sayeed, M. S. and Biondi, A. and Birihane, B. M. and Bisignano, C. and Biswas, R. K. and Bitew, H. and Bohlouli, S. and Bohluli, M. and Boon-Dooley, A. S. and Borges, G. and Borzì, A. M. and Borzouei, S. and Bosetti, C. and Boufous, S. and Braithwaite, D. and Breitborde, N. J. K. and Breitner, S. and Brenner, H. and Briant, P. S. and Briko, A. N. and Briko, N. I. and Britton, G. B. and Bryazka,

D. and Bumgarner, B. R. and Burkart, K. and Burnett, R. T. and Burugina Nagaraja, S. and Butt, Z. A. and Caetano Dos Santos, F. L. and Cahill, L. E. and Cámera, L. L. A. and Campos-Nonato, I. R. and Cárdenas, R. and Carreras, G. and Carrero, J. J. and Carvalho, F. and Castaldelli-Maia, J. M. and Castañeda-Orjuela, C. A. and Castelpietra, G. and Castro, F. and Causey, K. and Cederroth, C. R. and Cercy, K. M. and Cerin, E. and Chandan, J. S. and Chang, K.-L. and Charlson, F. J. and Chattu, V. K. and Chaturvedi, S. and Cherbuin, N. and Chimed-Ochir, O. and Cho, D. Y. and Choi, J.-Y. J. and Christensen, H. and Chu, D.-T. and Chung, M. T. and Chung, S.-C. and Cicuttini, F. M. and Ciobanu, L. G. and Cirillo, M. and Classen, T. K. D. and Cohen, A. J. and Compton, K. and Cooper, O. R. and Costa, V. M. and Cousin, E. and Cowden, R. G. and Cross, D. H. and Cruz, J. A. and Dahlawi, S. M. A. and Damasceno, A. A. M. and Damiani, G. and Dandona, L. and Dandona, R. and Dangel, W. J. and Danielsson, A.-K. and Dargan, P. I. and Darwesh, A. M. and Daryani, A. and Das, J. K. and Das Gupta, R. and Das Neves, J. and Dávila-Cervantes, C. A. and Davitoiu, D. V. and De Leo, D. and Degenhardt, L. and Delang, M. and Dellavalle, R. P. and Demeke, F. M. and Demoz, G. T. and Demsie, D. G. and Denova-Gutiérrez, E. and Dervenis, N. and Dhungana, G. P. and Dianatinasab, M. and Dias Da Silva, D. and Diaz, D. and Dibaji Forooshani, Z. S. and Djalalinia, S. and Do, H. T. and Dokova, K. and Dorostkar, F. and Doshmangir, L. and Driscoll, T. R. and Duncan, B. B. and Duraes, A. R. and Eagan, A. W. and Edvardsson, D. and El Nahas, N. and El Sayed, I. and El Tantawi, M. and Elbarazi, I. and Elgendy, I. Y. and El-Jaafary, S. I. and Elyazar, I. R. and Emmons-Bell, S. and Erskine, H. E. and Eskandarieh, S. and Esmaeilnejad, S. and Esteghamati, A. and Estep, K. and Etemadi, A. and Etisso, A. E. and Fanzo, J. and Farahmand, M. and Fareed, M. and Faridnia, R. and Farioli, A. and Faro, A. and Faruque, M. and Farzadfar, F. and Fattahi, N. and Fazlzadeh, M. and Feigin, V. L. and Feldman, R. and Fereshtehnejad, S.-M. and Fernandes, E. and Ferrara, G. and Ferrari, A. J. and Ferreira, M. L. and Filip, I. and Fischer, F. and Fisher, J. L. and Flor, L. S. and Foigt, N. A. and Folayan, M. O. and Fomenkov, A. A. and Force, L. M. and Foroutan, M. and Franklin, R. C. and Freitas, M. and Fu, W. and Fukumoto, T. and Furtado, J. M. and Gad, M. M. and Gakidou, E. and Gallus, S. and Garcia-Basteiro, A. L. and Gardner, W. M. and Geberemariyam, B. S. and Gebreslassie, A. A. A. A. and Geremew, A. and Gershberg Hayoon, A. and Gething, P. W. and Ghadimi, M. and Ghadiri, K. and Ghaffarifar, F. and Ghafourifard, M. and Ghamari, F. and Ghashghaee, A. and Ghiasvand, H. and Ghith, N. and Gholamian, A. and Ghosh, R. and Gill, P. S. and Ginindza, T. G. G. and Giussani, G. and Gnedovskaya, E. V. and Goharinezhad, S. and Gopalani, S. V. and Gorini, G. and Goudarzi, H. and Goulart, A. C. and Greaves, F. and Grivna, M. and Grosso, G. and Gubari, M. I. M. and Gugnani, H. C. and Guimarães, R. A. and Guled, R. A. and Guo, G. and Guo, Y. and Gupta, R. and Gupta, T. and Haddock, B. and Hafezi-Nejad, N. and Hafiz, A. and Haj-Mirzaian, A. and Haj-Mirzaian, A. and Hall, B. J. and Halvaei, I. and Hamadeh, R. R. and Hamidi, S. and Hammer, M. S. and Hankey, G. J. and Haririan, H. and Haro, J. M. and Hasaballah, A. I. and Hasan, M. M. and Hasanpoor, E. and Hashi, A. and Hassanipour, S. and Hassankhani, H. and Havmoeller, R. J. and Hay, S. I. and Hayat, K. and Heidari, G. and Heidari-Soureshjani, R. and Henrikson, H. J. and Herbert, M. E. and Herteliu, C. and Heydarpour, F. and Hird, T. R. and Hoek, H. W. and Holla, R. and Hoogar, P. and Hosgood, H. D. and Hossain, N. and Hosseini, M. and Hosseinzadeh, M. and Hostiuc, M. and Hostiuc, S. and Househ, M. and Hsairi, M. and Hsieh, V. C.-R. and Hu, G. and Hu, K. and Huda, T. M. and Humayun, A. and Huynh, C. K. and Hwang, B.-F. and Iannucci, V. C. and Ibitoye, S. E. and Ikeda, N. and Ikuta, K. S. and Ilesanmi, O. S. and Ilic, I. M. and Ilic, M. D. and Inbaraj, L. R. and Ippolito, H. and Iqbal, U. and Irvani, S. S. N. and Irvine, C. M. S. and Islam, M. M. and Islam, S. M. S. and Iso, H. and Ivers, R. Q. and Iwu, C. C. D. and Iwu, C. J. and Iyamu, I. O. and Jaafari, J. and Jacobsen, K. H. and Jafari, H. and Jafarinia, M. and Jahani, M. A. and Jakovljevic, M. and Jalilian, F. and James, S. L. and Janjani, H. and Javaheri, T. and Javidnia, J. and Jeemon, P. and Jenabi, E. and Jha, R. P. and Jha, V. and Ji, J. S. and Johansson, L. and John, O. and John-Akinola, Y. O. and Johnson, C. O. and Jonas, J. B. and Joukar, F. and Jozwiak, J. J. and Jürisson, M. and Kabir, A. and Kabir, Z. and Kalani, H. and Kalani, R. and Kalankesh, L. R. and Kalhor, R. and Kanchan, T. and Kapoor, N. and Karami Matin, B. and Karch, A. and Karim, M. A. and Kassa, G. M. and Katikireddi, S. V. and Kayode, G. A. and Kazemi Karyani, A. and Keiyoro, P. N. and Keller, C. and Kemmer, L. and Kendrick, P. J. and Khalid, N. and Khammarnia, M. and Khan, E. A. and Khan, M. and Khatab, K. and Khater, M. M. and Khatib, M. N. and Khayamzadeh, M. and Khazaei, S. and Kieling, C. and Kim, Y. J. and Kimokoti, R. W. and Kisa, A. and Kisa, S. and Kivimäki, M. and Knibbs, L. D. and Knudsen, A. K. S. and Kocarnik, J. M. and Kochhar, S. and Kopec, J. A. and Korshunov, V. A. and Koul, P. A. and Koyanagi, A. and Kraemer, M. U. G. and Krishan, K. and Krohn, K. J. and Kromhout, H. and Kuate Defo, B. and Kumar, G. A. and Kumar, V. and Kurmi, O. P. and Kusuma, D. and La Vecchia, C. and Lacey, B. and Lal, D. K. and Lalloo, R. and Lallukka, T. and Lami, F. H. and Landires, I. and Lang, J. J. and Langan, S. M. and Larsson, A. O. and Lasrado, S. and Lauriola, P. and Lazarus, J. V. and Lee, P. H. and Lee, S. W. H. and Legrand, K. E. and Leigh, J. and Leonardi, M. and Lescinsky, H. and Leung, J. and Levi, M. and Li, S. and Lim, L.-L. and Linn, S. and Liu, S. and Liu, S. and Liu, Y. and Lo, J. and Lopez, A. D. and Lopez, J. C. F. and Lopukhov, P. D. and Lorkowski, S. and Lotufo, P. A. and Lu, A. and Lugo, A. and Maddison, E. R. and Mahasha, P. W. and Mahdavi, M. M. and Mahmoudi, M. and Majeed, A. and Maleki, A. and Maleki, S. and Malekzadeh, R. and Malta, D. C. and Mamun, A. A. and Manda, A. L. and Manguerra, H. and Mansour-Ghanaei, F. and Mansouri, B. and Mansournia, M. A. and Mantilla Herrera, A. M. and Maravilla, J. C. and Marks, A. and Martin, R. V. and Martini, S. and Martins-Melo, F. R. and Masaka, A. and Masoumi, S. Z. and Mathur, M. R. and Matsushita, K. and Maulik, P. K. and McAlinden, C. and McGrath, J. J. and McKee, M. and Mehndiratta, M. M. and Mehri, F. and Mehta, K. M. and Memish, Z. A. and Mendoza, W. and Menezes, R. G. and Mengesha, E. W. and Mereke, A. and Mereta, S. T. and Meretoja, A. and Meretoja, T. J. and Mestrovic, T. and Miazgowski, B. and Miazgowski, T. and Michalek, I. M. and Miller, T. R. and Mills, E. J. and Mini, G. and Miri, M. and Mirica, A. and Mirrakhimov, E. M. and Mirzaei, H. and Mirzaei, M. and Mirzaei, R. and Mirzaei-Alavijeh, M. and Misganaw, A. T. and Mithra, P. and Moazen, B. and Mohammad, D. K. and Mohammad, Y. and Mohammad Gholi Mezerji, N. and Mohammadian-Hafshejani, A. and Mohammadifard, N.

and Mohammadpourhodki, R. and Mohammed, A. S. and Mohammed, H. and Mohammed, J. A. and Mohammed, S. and Mokdad, A. H. and Molokhia, M. and Monasta, L. and Mooney, M. D. and Moradi, G. and Moradi, M. and Moradi-Lakeh, M. and Moradzadeh, R. and Moraga, P. and Morawska, L. and Morgado-Da-Costa, J. and Morrison, S. D. and Mosapour, A. and Mosser, J. F. and Mouodi, S. and Mousavi, S. M. and Mousavi Khaneghah, A. and Mueller, U. O. and Mukhopadhyay, S. and Mullany, E. C. and Musa, K. I. and Muthupandian, S. and Nabhan, A. F. and Naderi, M. and Nagarajan, A. J. and Nagel, G. and Naghavi, M. and Naghshtabrizi, B. and Naimzada, M. D. and Najafi, F. and Nangia, V. and Nansseu, J. R. and Naserbakht, M. and Nayak, V. C. and Negoi, I. and Ngunjiri, J. W. and Nguyen, C. T. and Nguyen, H. L. T. and Nguyen, M. and Nigatu, Y. T. and Nikbakhsh, R. and Nixon, M. R. and Nnaji, C. A. and Nomura, S. and Norrving, B. and Noubiap, J. J. and Nowak, C. and Nunez-Samudio, V. and Oţoiu, A. and Oancea, B. and Odell, C. M. and Ogbo, F. A. and Oh, I.-H. and Okunga, E. W. and Oladnabi, M. and Olagunju, A. T. and Olusanya, B. O. and Olusanya, J. O. and Omer, M. O. and Ong, K. L. and Onwujekwe, O. E. and Orpana, H. M. and Ortiz, A. and Osarenotor, O. and Osei, F. B. and Ostroff, S. M. and Otstavnov, N. and Otstavnov, S. S. and Øverland, S. and Owolabi, M. O. and P A, M. and Padubidri, J. R. and Palladino, R. and Panda-Jonas, S. and Pandey, A. and Parry, C. D. H. and Pasovic, M. and Pasupula, D. K. and Patel, S. K. and Pathak, M. and Patten, S. B. and Patton, G. C. and Pazoki Toroudi, H. and Peden, A. E. and Pennini, A. and Pepito, V. C. F. and Peprah, E. K. and Pereira, D. M. and Pesudovs, K. and Pham, H. Q. and Phillips, M. R. and Piccinelli, C. and Pilz, T. M. and Piradov, M. A. and Pirsaheb, M. and Plass, D. and Polinder, S. and Polkinghorne, K. R. and Pond, C. D. and Postma, M. J. and Pourjafar, H. and Pourmalek, F. and Poznańska, A. and Prada, S. I. and Prakash, V. and Pribadi, D. R. A. and Pupillo, E. and Quazi Syed, Z. and Rabiee, M. and Rabiee, N. and Radfar, A. and Rafiee, A. and Raggi, A. and Rahman, M. A. and Rajabpour-Sanati, A. and Rajati, F. and Rakovac, I. and Ram, P. and Ramezanzadeh, K. and Ranabhat, C. L. and Rao, P. C. and Rao, S. J. and Rashedi, V. and Rathi, P. and Rawaf, D. L. and Rawaf, S. and Rawal, L. and Rawassizadeh, R. and Rawat, R. and Razo, C. and Redford, S. B. and Reiner, R. C. and Reitsma, M. B. and Remuzzi, G. and Renjith, V. and Renzaho, A. M. N. and Resnikoff, S. and Rezaei, N. and Rezaei, N. and Rezapour, A. and Rhinehart, P.-A. and Riahi, S. M. and Ribeiro, D. C. and Ribeiro, D. and Rickard, J. and Rivera, J. A. and Roberts, N. L. S. and Rodríguez-Ramírez, S. and Roever, L. and Ronfani, L. and Room, R. and Roshandel, G. and Roth, G. A. and Rothenbacher, D. and Rubagotti, E. and Rwegerera, G. M. and Sabour, S. and Sachdev, P. S. and Saddik, B. and Sadeghi, E. and Sadeghi, M. and Saeedi, R. and Saeedi Moghaddam, S. and Safari, Y. and Safi, S. and Safiri, S. and Sagar, R. and Sahebkar, A. and Sajadi, S. M. and Salam, N. and Salamati, P. and Salem, H. and Salem, M. R. R. and Salimzadeh, H. and Salman, O. M. and Salomon, J. A. and Samad, Z. and Samadi Kafil, H. and Sambala, E. Z. and Samy, A. M. and Sanabria, J. and Sánchez-Pimienta, T. G. and Santomauro, D. F. and Santos, I. S. and Santos, J. V. and Santric-Milicevic, M. M. and Saraswathy, S. Y. I. and Sarmiento-Suárez, R. and Sarrafzadegan, N. and Sartorius, B. and Sarveazad, A. and Sathian, B. and Sathish, T. and Sattin, D. and Saxena, S. and Schaeffer, L. E. and Schiavolin, S. and Schlaich, M. P. and Schmidt, M. I. and Schutte, A. E. and Schwebel, D. C. and Schwendicke, F. and Senbeta, A. M. and Senthilkumaran, S. and Sepanlou, S. G. and Serdar, B. and Serre, M. L. and Shadid, J. and Shafaat, O. and Shahabi, S. and Shaheen, A. A. and Shaikh, M. A. and Shalash, A. S. and Shams-Beyranvand, M. and Shamsizadeh, M. and Sharafi, K. and Sheikh, A. and Sheikhtaheri, A. and Shibuya, K. and Shield, K. D. and Shigematsu, M. and Shin, J. I. and Shin, M.-J. and Shiri, R. and Shirkoohi, R. and Shuval, K. and Siabani, S. and Sierpinski, R. and Sigfusdottir, I. D. and Sigurvinsdottir, R. and Silva, J. P. and Simpson, K. E. and Singh, J. A. and Singh, P. and Skiadaresi, E. and Skou, S. T. and Skryabin, V. Y. and Smith, E. U. R. and Soheili, A. and Soltani, S. and Soofi, M. and Sorensen, R. J. D. and Soriano, J. B. and Sorrie, M. B. and Soshnikov, S. and Soyiri, I. N. and Spencer, C. N. and Spotin, A. and Sreeramareddy, C. T. and Srinivasan, V. and Stanaway, J. D. and Stein, C. and Stein, D. J. and Steiner, C. and Stockfelt, L. and Stokes, M. A. and Straif, K. and Stubbs, J. L. and Sufiyan, M. A. B. and Suleria, H. A. R. and Suliankatchi Abdulkader, R. and Sulo, G. and Sultan, I. and Szumowski, Ł. and Tabarés-Seisdedos, R. and Tabb, K. M. and Tabuchi, T. and Taherkhani, A. and Tajdini, M. and Takahashi, K. and Takala, J. S. and Tamiru, A. T. and Taveira, N. and Tehrani-Banihashemi, A. and Temsah, M.-H. and Tesema, G. A. and Tessema, Z. T. and Thurston, G. D. and Titova, M. V. and Tohidinik, H. R. and Tonelli, M. and Topor-Madry, R. and Topouzis, F. and Torre, A. E. and Touvier, M. and Tovani-Palone, M. R. R. and Tran, B. X. and Travillian, R. and Tsatsakis, A. and Tudor Car, L. and Tyrovolas, S. and Uddin, R. and Umeokonkwo, C. D. and Unnikrishnan, B. and Upadhyay, E. and Vacante, M. and Valdez, P. R. and Van Donkelaar, A. and Vasankari, T. J. and Vasseghian, Y. and Veisani, Y. and Venketasubramanian, N. and Violante, F. S. and Vlassov, V. and Vollset, S. E. and Vos, T. and Vukovic, R. and Waheed, Y. and Wallin, M. T. and Wang, Y. and Wang, Y.-P. and Watson, A. and Wei, J. and Wei, M. Y. W. and Weintraub, R. G. and Weiss, J. and Werdecker, A. and West, J. J. and Westerman, R. and Whisnant, J. L. and Whiteford, H. A. and Wiens, K. E. and Wolfe, C. D. A. and Wozniak, S. S. and Wu, A.-M. and Wu, J. and Wulf Hanson, S. and Xu, G. and Xu, R. and Yadgir, S. and Yahyazadeh Jabbari, S. H. and Yamagishi, K. and Yaminfirooz, M. and Yano, Y. and Yaya, S. and Yazdi-Feyzabadi, V. and Yeheyis, T. Y. and Yilgwan, C. S. and Yilma, M. T. and Yip, P. and Yonemoto, N. and Younis, M. Z. and Younker, T. P. and Yousefi, B. and Yousefi, Z. and Yousefinezhadi, T. and Yousuf, A. Y. and Yu, C. and Yusefzadeh, H. and Zahirian Moghadam, T. and Zamani, M. and Zamanian, M. and Zandian, H. and Zastrozhin, M. S. and Zhang, Y. and Zhang, Z.-J. and Zhao, J. T. and Zhao, X.-J. G. and Zhao, Y. and Zhou, M. and Ziapour, A. and Zimsen, S. R. M. and Brauer, M. and Afshin, A. and Lim, S. S.: Global burden of 87 risk factors in 204 countries and territories, 1990–2019: a systematic analysis for the Global Burden of Disease Study 2019, The Lancet, 396, 1223-1249, 10.1016/s0140-6736(20)30752-2, 2020.

Nenes, A., Pandis, S. N., and Pilinis, C.: ISORROPIA: A New Thermodynamic Equilibrium Model for Multiphase Multicomponent Inorganic Aerosols, Aquatic Geochemistry, 4, 123-152, 10.1023/a:1009604003981, 1998.

Ng, N. L., Kwan, A. J., Surratt, J. D., Chan, A. W. H., Chhabra, P. S., Sorooshian, A., Pye, H. O. T., Crounse, J. D., Wennberg, P. O., Flagan, R. C., and Seinfeld, J. H.: Secondary organic aerosol (SOA) formation from reaction of isoprene with nitrate radicals (NO₃), Atmospheric Chemistry and Physics, 8, 4117-4140, 10.5194/acp-8-4117-2008, 2008.

Pellegrini, E. and Russell, R. P.: On the Computation and Accuracy of Trajectory State Transition Matrices, Journal of Guidance, Control, and Dynamics, 39, 2485-2499, 10.2514/1.G001920, 2016.

Pilinis, C., Capaldo, K. P., Nenes, A., and Pandis, S. N.: MADM-A New Multicomponent Aerosol Dynamics Model, Aerosol Science and Technology, 32, 482-502, 10.1080/027868200303597, 2000.

Ring, A. M., Canty, T. P., Anderson, D. C., Vinciguerra, T. P., He, H., Goldberg, D. L., Ehrman, S. H., Dickerson, R. R., and Salawitch, R. J.: Evaluating commercial marine emissions and their role in air quality policy using observations and the CMAQ model, Atmospheric Environment, 173, 96-107, https://doi.org/10.1016/j.atmosenv.2017.10.037, 2018.

Sandu, A., Daescu, D. N., Carmichael, G. R., and Chai, T.: Adjoint sensitivity analysis of regional air quality models, Journal of Computational Physics, 204, 222-252, 2005.

Sareen, N., Carlton, A. G., Surratt, J. D., Gold, A., Lee, B., Lopez-Hilfiker, F. D., Mohr, C., Thornton, J. A., Zhang, Z., Lim, Y. B., and Turpin, B. J.: Identifying precursors and aqueous organic aerosol formation pathways during the SOAS campaign, Atmospheric Chemistry and Physics, 16, 14409-14420, 10.5194/acp-16-14409-2016, 2016.

Sayeed, A., Lops, Y., Choi, Y., Jung, J., and Salman, A. K.: Bias correcting and extending the PM forecast by CMAQ up to 7 days using deep convolutional neural networks, Atmospheric Environment, 253, 118376, https://doi.org/10.1016/j.atmosenv.2021.118376, 2021.

Squire, W. and Trapp, G.: Using Complex Variables to Estimate Derivatives of Real Functions, SIAM Review, 40, 110-112, 10.1137/s003614459631241x, 1998.

Tian, D., Cohan, D. S., Napelenok, S., Bergin, M., Hu, Y., Chang, M., and Russell, A. G.: Uncertainty Analysis of Ozone Formation and Response to Emission Controls Using Higher-Order Sensitivities, Journal of the Air & Waste Management Association, 60, 797-804, 10.3155/1047-3289.60.7.797, 2010.

U.S. Environmental Protection Agency: CMAQ Model Version 5.3, 5.3.1, 5.3.2, 5.3.3 Input Data -- 7/1/2016 - 7/14/2016 12km Southeast US (V1), UNC Dataverse [dataset], doi:10.15139/S3/IQVABD, 2019.

U.S. Environmental Protection Agency: CMAQ (Version 5.3.2) [code], 2020.

Wong, D. C., Yang, C. E., Fu, J. S., Wong, K., and Gao, Y.: An approach to enhance pnetCDF performance in environmental modeling applications, Geosci. Model Dev., 8, 1033-1046, 10.5194/gmd-8-1033-2015, 2015.

Xu, L., Pye, H. O. T., He, J., Chen, Y., Murphy, B. N., and Ng, N. L.: Experimental and model estimates of the contributions from biogenic monoterpenes and sesquiterpenes to secondary organic aerosol in the southeastern United States, Atmospheric Chemistry and Physics, 18, 12613-12637, 10.5194/acp-18-12613-2018, 2018.

Zhang, W., Capps, S. L., Hu, Y., Nenes, A., Napelenok, S. L., and Russell, A. G.: Development of the high-order decoupled direct method in three dimensions for particulate matter: enabling advanced sensitivity analysis in air quality models, Geoscientific Model Development, 5, 355-368, 10.5194/gmd-5-355-2012, 2012.

Zhao, S., Russell, M. G., Hakami, A., Capps, S. L., Turner, M. D., Henze, D. K., Percell, P. B., Resler, J., Shen, H., Russell, A. G., Nenes, A., Pappin, A. J., Napelenok, S. L., Bash, J. O., Fahey, K. M., Carmichael, G. R., Stanier, C. O., and Chai, T.: A multiphase CMAQ version 5.0 adjoint, Geoscientific Model Development, 13, 2925-2944, 10.5194/gmd-13-2925-2020, 2020.

Zhu, S., Horne, J. R., Montoya-Aguilera, J., Hinks, M. L., Nizkorodov, S. A., and Dabdub, D.: Modeling reactive ammonia uptake by secondary organic aerosol in CMAQ: application to the continental US, Atmospheric Chemistry and Physics, 18, 3641-3657, 10.5194/acp-18-3641-2018, 2018.